1.D.2 *Nuclear Physics* **A234** (1974) 216—252; © *North-Holland Publishing Co., Amsterdam*

GENERALIZED NEUTRON PARTICLE-HOLE STATES IN AN EXTENDED UNIFIED MODEL

K. HEYDE, M. WAROQUIER † and H. VINCX ††
Natuurkundig Laboratorium, INW, Proeftuinstraat 86, B-9000 Gent, Belgium
and
P. J. BRUSSAARD
Fysisch Laboratorium, Sorbonnelaan 4, Utrecht, The Netherlands

Received 29 March 1974
(Revised 4 July 1974)

Abstract: Negative-parity levels in the doubly even $N = 82$, Z nuclei, with 3.0 MeV $\lessapprox E_x \lessapprox$ 6.0 MeV are described in an extended unified-model approach, where neutron hole states in the $Z = 50$, $N = 82$ closed shell core, (i.e. $2d_{\frac{3}{2}}^{-1}$, $3s_{\frac{1}{2}}^{-1}$, $2d_{\frac{5}{2}}^{-1}$, $1g_{\frac{7}{2}}^{-1}$) are coupled to the low-lying levels ($E_x \lessapprox$ 2.0 MeV) of the odd-neutron $N = 83$, Z nuclei. This particular configuration space of generalized neutron particle-hole states (GNPH) is particularly suited for describing negative-parity levels obtained in proton inelastic scattering through isobaric analogue resonances (IAR), corresponding to the $N = 83$, Z low-lying nuclear levels. Level schemes as well as partial decay widths and angular distributions are calculated and compared extensively with the available experimental data. Also spectroscopic factors, as well as wave functions, deduced from the experimental results are studied in detail. Thus in the cases of ^{136}Xe, ^{138}Ba, ^{140}Ce, ^{142}Nd and ^{144}Sm, some of the important neutron particle-hole configurations can uniquely be determined in the energy region 3.0 MeV $\lessapprox E_x \lessapprox$ 6.0 MeV.

1. Introduction

Nuclear levels in the $N = 81$ and $N = 83$ nuclei have been calculated in a weak-coupling picture originally suggested by Bohr and Mottelson [1]), with the assumption of a shell closure at $N = 82$ [ref. [2])]. Results from elastic proton scattering through isobaric analogue resonances (IAR) [3-13]) as well as from neutron transfer reactions [refs. [14-18])] are consistent with a weak-coupling idea of describing ground state and low-lying levels ($E_x \lessapprox$ 2.0 MeV) in the $N = 81$ and $N = 83$ nuclei. Nuclear-structure information concerning higher lying levels in the doubly even $N = 82$ nuclei (3.0 MeV $< E_x <$ 6.0 MeV) can be obtained from inelastic proton scattering through IAR [19-32]), (d, t) and (d, p) reactions in the $N = 83$ and $N = 81$ nuclei, respectively. The negative-parity levels thus obtained in the doubly even $N = 82$ nuclei are fed selectively in (p, p′) reactions on separate resonances, suggesting a weak-coupling description, in which neutron hole states are coupled to the low-lying $N = 83$ nu-

† "Aangesteld navorser" of the NFWO.
†† "Aspirant" of the NFWO.

clear levels. For the $N = 83$ nuclei, as well as for the $N = 81$ nuclei, a unified-model description has been given [2, 33]) where the properties of the low-lying states are discussed. The calculation of partial decay widths from the IAR to negative-parity levels in the doubly even $N = 82$, Z nuclei and of angular distributions for the inelastically scattered protons through IAR, can be used as a better test of the wave functions. Calculation of these observables can also be used to identify the rather pure generalized neutron particle-hole (GNPH) states among the excited negative-parity levels observed experimentally. In sect. 2 we construct the wave function describing the IAR states in an extended unified model (EUM) and study the possible decay modes, with special application to ^{140}Ce as well as the necessary formulae to study angular distributions of inelastically scattered protons. In sect. 3 the EUM is developed further in order to describe negative-parity levels in the doubly even $N = 82$ nuclei and the parameters occurring in the model are also discussed. In sect. 4 application is made to the level schemes, partial decay widths, angular distributions and spectroscopic factors of the doubly even $N = 82$ nuclei, in the energy region 3.0 MeV $< E_x <$ 6.0 MeV. Finally, conclusions are drawn about the existence of the GNPH multiplets in the doubly even $N = 82$ isotones, and on the validity of a weak-coupling picture for coupling neutron hole states to the parent ($N = 83$, Z) low-lying levels.

2. IAR wave function

2.1. UNIFIED-MODEL DESCRIPTION

Assuming a unified-model description for the low-lying levels in the $N = 83$ nuclei, one can describe each state as

$$|N = 83, Z; J_\beta M\rangle = c_\beta(J, 00; J)a^+_{JM}(\nu)|\tilde{0}\rangle + \sum_{j_p, N\geqq 1, R} c_\beta(j_p, NR; J)[a^+_{j_p}(\nu) \otimes \Omega^+_{NR}]_{JM}|\tilde{0}\rangle, \tag{2.1}$$

where $|\tilde{0}\rangle$ represents the vacuum state given by the physical ground state of the $N = 82$, Z nucleus, β distinguishes different states of the same value J, $a^+_{jm}(\nu)$ creates a neutron in the single-particle state (j, m) and $\Omega^+_{NRM_R}$ creates an N quadrupole phonon state with angular momentum R and projection M_R. The expansion coefficients $c_\beta(j_p, NR; J)$ are obtained after diagonalizing the particle-core interaction [2]) for states of spin J in the $N = 83$ nuclei. The isobaric analogues of these low-lying levels can be given as

$$|N = 82, Z+1; J_\beta M\rangle_{(A)} = (2T_0+1)^{-\frac{1}{2}}\{c_\beta(J, 00; J)a^+_{JM}(\pi)|\tilde{0}\rangle + \sum_{j_p, N\geqq 1, R} c_\beta(j_p, NR; J)[a^+_{j_p}(\pi) \otimes \Omega^+_{NR}]_{JM}|\tilde{0}\rangle + \sum_{j_h, I}\left(\frac{2I+1}{2J+1}\right)^{\frac{1}{2}} \times(-1)^{j_h+J-I}[a^+_{j_h}(\pi) \otimes [\tilde{a}_{j_h}(\nu) \otimes |N = 83, Z; J_\beta\rangle]_I]_{JM}\}, \tag{2.2}$$

where j_p has to be summed over the angular momenta of the shell-model states above the $N = 82$ closed shell and j_h over the shells below the $N = 82$ closed shell; $a^+_{jm}(\pi)$ creates a proton in the single-particle state (j, m), the isospin of the $N = 82$, Z core is denoted by T_0 and the time-reversed annihilation operator is given by $\tilde{a}_{jm} \equiv (-1)^{j+m} a_{j,-m}$.

2.2. DECAY MODES

The three components in eq. (2.2) correspond to different proton decay modes of the IAR to levels in the final doubly even $N = 82$, Z nuclei.

(i) The first term describes decay in the proton elastic channel by emission of a proton in the single-particle orbit J, M. The partial decay width is calculated as

$$\Gamma^{\mathrm{el}}_{J_\beta} = \Gamma^{\mathrm{s.p.}}_J \frac{1}{2T_0+1} |c_\beta(J, 00; J)|^2, \tag{2.3}$$

where $\Gamma^{\mathrm{s.p.}}_J$ denotes the decay width for a hypothetical analogue resonance of pure single-nucleon character [36]). A spectroscopic factor for elastic proton scattering can be defined by

$$\Gamma^{\mathrm{el}}_{J_\beta} = \Gamma^{\mathrm{s.p.}}_J S_{\mathrm{p,p}}(J_\beta). \tag{2.4}$$

Thus with the calculated values of $\Gamma^{\mathrm{s.p.}}_J$, spectroscopic factors can be deduced from the experimental data and be compared to the spectroscopic factor $S_{\mathrm{d,p}}$ obtained in neutron stripping to the final $N = 83$ nuclei. In table 1, a comparison is made between $S_{\mathrm{p,p}}$, $S_{\mathrm{d,p}}$ and the theoretical values as calculated from eq. (2.1) in a unified-model description for the nuclues ^{141}Ce.

TABLE 1

The spectroscopic factors as obtained from neutron stripping reactions ($S_{\mathrm{d,p}}$), compared to spectroscopic factors from elastic proton scattering ($S_{\mathrm{p,p}}$) and the theoretical values, given by $|c_\beta(j_p, 00; j_p)|^2$ in ^{141}Ce

E_x (MeV)	J^π	l	$S_{\mathrm{d,p}}$		$S_{\mathrm{p,p}}$			Theory
			[a])	[b])	[c])	[d])	[e])	
0.0	$\frac{7}{2}^-$	3	0.89	0.74	0.86	0.86	0.67	0.88
0.66	$\frac{3}{2}^-$	1	0.42	0.55	0.42	0.42	0.29	0.51
1.14	$\frac{1}{2}^-$	1	0.38	0.66	0.28	0.28	0.25	0.62
1.37	$\frac{9}{2}^-$	5	1.20		(0.6)			0.52
1.38								0.33
1.50	$\frac{5}{2}^-$	3	0.30	0.30	0.27	0.27	0.23	0.27
1.69	$\frac{7}{2}^-$	3		0.15				0.08
1.74	$\frac{5}{2}^-$	3	0.38	0.26	0.25	0.25	0.22	0.30
1.81	$\frac{3}{2}^-$	1		0.12				0.30
1.98								0.22

[a]) Ref. [16]). [b]) Ref. [35]). [c]) Ref. [5]). [d]) Ref. [36]). [e]) Ref. [34]).

(ii) The second term describes decay to phonon excitations $\Omega_{NR}^{+}|\tilde{0}\rangle$ of the $N = 82$, Z core nucleus, which can be identified – at least for the one-phonon state $I_\alpha^\pi = 2_1^+$ – with pure proton excitations [37]). Decay to the highly collective $I_\alpha^\pi = 2_{(1)}^+$ state gives as the partial decay width

$$\Gamma_{J_\beta}^{\text{inel}}(2_1^+) = \sum_{j_p} \Gamma_{j_p}^{\text{s.p.}} \frac{1}{2T_0+1} |c_\beta(j_p, 12; J)|^2. \tag{2.5}$$

These experimental, inelastic (p, p′)$2_{(1)}^+$ data [38, 39]) are a severe test for the unified-model description of the $N = 83$ nuclei, in which the lowest single-neutron excitations are coupled to the $I_\alpha^\pi = 2_{(1)}^+$ quadrupole vibrational state of the core. In table 2, the theoretical amplitudes $c_\beta(j_p, 12; J)$ are given for the lowest six excited states in ^{141}Ce and compared to the experimental results as obtained from the Erlangen group [38, 39]).

TABLE 2

The amplitudes $c_\beta(lj_p, I_\alpha^\pi; J^\pi)$ from unified-model calculations, compared to the experimental amplitudes obtained from inelastic polarized-proton scattering on ^{140}Ce (theoretical values given between brackets)

$E_x(\beta)$ (MeV)	J_β^π	$c_\beta(lj, I_\alpha^\pi; J^\pi)$					$\sum_{I,j,l} c_\beta^2$
		$I_\alpha^\pi = 0_1^+$ (g.s.)	$I_\alpha^\pi = 2_1^+$ ($E_x = 1.596$ MeV)				
		$j = j_\lambda$	$3p_{\frac{1}{2}}$	$3p_{\frac{3}{2}}$	$2f_{\frac{5}{2}}$	$2f_{\frac{7}{2}}$	
0.66	$\frac{3}{2}^-_{(1)}$	0.63	−0.12	−0.12	−0.05	−0.61	0.80
		(0.72)	(−0.15)	(−0.20)	(−0.08)	(−0.60)	
1.14	$\frac{1}{2}^-_{(1)}$	0.49		0.34	−0.43		0.55
		(0.79)		(0.44)	(−0.29)		
1.53	$\frac{5}{2}^-_{(1)}$	0.55	−0.29	−0.17	−0.41	0.51	0.85
		(0.52)	(−0.18)	(0.17)	(−0.15)	(0.70)	
1.79	$\frac{7}{2}^-_{(2)}$	0.33		0.21	−0.47	0.73	0.91
		(0.28)		(−0.04)	(−0.02)	(0.87)	
1.86	$\frac{3}{2}^-_{(2)}$	0.32	0.26	−0.13	−0.23	0.23	0.31
		(0.55)	(0.17)	(−0.26)	(−0.06)	(0.71)	
1.88	$\frac{5}{2}^-_{(2)}$	0.49	0.12	0.22	0.06	−0.33	0.41
		(0.53)	(0.22)	(0.19)	(−0.17)	(−0.67)	

(iii) The third term describes the decay to configurations that show a neutron hole in the physical $N = 82$, Z core state. These configurations $[\tilde{a}_{j_h}(\nu)\otimes|N = 83, Z; J_\beta\rangle]_{IM}$ are referred to as generalized neutron particle-hole states (GNPH). In general they contain in addition to a neutron-particle-neutron-hole configuration, also more complicated admixtures that derive from the collective excitations involved. They form a complete set for the expansion of the $N = 82$, Z states.

Experiments at Heidelberg [22–28]), the University of Texas [19, 20]), ANL [21]) and the University of Montreal [29–32]), show a quite selective feeding of higher-lying (3.5 MeV $< E_I^{(\alpha)} <$ 6.0 MeV), negative-parity levels in inelastic proton scattering.

Neutron-hole excitations should be present in these final states, that can be reached by proton emission from the third component of eq. (2.2). Expanding the final states in terms of the GNPH, one obtains

$$|N = 82, Z; I_\alpha M\rangle = \sum_{j_h, J, \beta} d_\alpha(j_h, J_\beta; I) \times [\tilde{a}_{j_h}(\nu) \otimes |N = 83, Z; J_\beta\rangle]_{IM}. \tag{2.6}$$

The third component of eq. (2.2) can be rewritten as

$$(2T_0+1)^{-\frac{1}{2}} \sum_{j_h, I, \alpha} \left(\frac{2I+1}{2J+1}\right)^{\frac{1}{2}} (-1)^{j_h+J-I} d_\alpha(j_h, J_\beta; I) \times [a^+_{j_h}(\pi) \otimes |N = 82, Z; I_\alpha\rangle]_{IM}. \tag{2.7}$$

The partial decay width to a final level I_α then becomes

$$\Gamma^{\text{inel}}_{J_\beta}(I_\alpha) = \sum_{j_h} \frac{2I+1}{(2J+1)(2T_0+1)} \Gamma^{\text{s.p.}}_{j_h} |d_\alpha(j_h, J_\beta; I)|^2. \tag{2.8}$$

Through the experimental determination of angular distributions the emission of d- or s-wave protons can be distinguished and even the separate amplitudes $d_\alpha(j_h, J_\beta; I)$ can be obtained [23, 28]).

2.3. ANGULAR DISTRIBUTIONS

The differential cross section for proton scattering from an $I^\pi = 0^+$ ground state, through a resonance J_β, is given by [24])

$$\frac{d\sigma}{d\Omega}(\theta)[0^+ \underset{(l_0, J_\beta)}{\rightarrow} I_\alpha] = \frac{\Gamma^2_{\text{tot}}(J_\beta)}{4(E - E_{\text{res}}(J_\beta))^2 + \Gamma^2_{\text{tot}}(J_\beta)} \times \sum_{k=0(\text{even})}^{k_{\max}} a_k^{I_\alpha J_\beta} P_k(\cos\theta), \tag{2.9}$$

with

$$a_k^{I_\alpha J_\beta} = \frac{1}{4\pi} \Lambda_{J_\beta} \sum_{r,s} d_\alpha(j_r, J_\beta; I) A_k^{I_\alpha J_\beta}(r, s) d_\alpha(j_s, J_\beta; I), \tag{2.10}$$

$$\Lambda_{J_\beta} = \frac{\hbar^2 \pi}{\mu_0} \frac{2J+1}{E_{\text{res}}(J_\beta)} \frac{\Gamma^{\text{el}}_{J_\beta}}{\Gamma^2_{\text{tot}}(J_\beta)}, \tag{2.11}$$

$$A_k^{I_\alpha J_\beta}(r, s) = (-1)^{I+2J} \frac{2I+1}{2J+1} W(j_r J j_s J; Ik) \times \bar{Z}(l_0 J l_0 J; \tfrac{1}{2}k) \bar{Z}(l_r j_r l_s j_s; \tfrac{1}{2}k) (\Gamma^{\text{s.p.}}_{l_r j_r} \Gamma^{\text{s.p.}}_{l_s j_s})^{\frac{1}{2}} \times \cos(\xi^{\text{s.p.}}_{l_r j_r} - \xi^{\text{s.p.}}_{l_s j_s}). \tag{2.12}$$

Here $\Gamma^{\text{s.p.}}_{lj}$ and $\xi^{\text{s.p.}}_{lj}$ denote the single-particle width and single-particle phase respectively. The elastic width for the resonance J_β is given by $\Gamma^{\text{el}}_{J_\beta}$ and the total width by $\Gamma_{\text{tot}}(J_\beta)$. The W and $\bar{Z}$ coefficients are defined in ref. [40]).

After integrating eq. (2.9), one obtains on top of the resonance

$$\sigma_{J_\beta}(0^+ \to I_\alpha) = 4\pi a_0^{I_\alpha J_\beta}. \tag{2.13}$$

The single-particle phases have been calculated with the program HANS [41]), which is based upon the method of Zaidi, Darmodjo [10]) and Harney [36]). The amplitudes $d_\alpha(lj, J_\beta; I)$ are obtained in the GNPH model. Calculating and studying the angular distributions and their systematic behaviour in detail, one can obtain a better understanding of the high-lying negative-parity states in the doubly even $N = 82$ isotones.

3. The extended unified model (EUM)

3.1. HAMILTONIAN

For a description of the wave functions for the final states in the doubly even $N = 83$, Z nuclei with negative parity and neutron particle-hole nature, one can construct a model Hamiltonian in terms of a weak coupling of a neutron-hole state to the low-lying levels in the $N = 83$, Z nuclei. One could, however, also couple neutron-particle states to the low-lying levels in the $N = 81$, Z-nuclei.

The first alternative turns out to the best suited for a description of the levels that are observed in proton inelastic scattering through IAR in doubly even $N = 82$, Z nuclei (see appendix A). The total Hamiltonian can be written as

$$H = H_c + H_p + H_h + H_{p-c} + H_{h-c} + V_{p-h}, \tag{3.1}$$

where H_c describes the low-lying collective excitations of the $N = 82$, Z-core, $H_p(H_h)$ the neutron single-particle ($-$hole) states, $H_{p-c}(H_{h-c})$ the interaction of the particle (hole) motion with the surface vibrations of the core and V_{p-h} the residual particle-hole interaction. The residual interaction Hamiltonian can be rewritten more explicitly, in second quantization, as

$$H_{\text{res}} = \sum_{\mu,\alpha,\beta} \xi_2 (b_{2\mu} + (-1)^\mu b^+_{2,-\mu}) \langle \alpha | Y_{2\mu} | \beta \rangle N(a^+_\alpha a_\beta) + \sum_{\alpha,\beta,\gamma,\delta} \langle \alpha\beta | V | \gamma\delta \rangle_{\text{a.s.}} N(a^+_\alpha a^+_\beta a_\delta a_\gamma), \tag{3.2}$$

where the normal product $N(\ldots)$ is defined with respect to the core ground state $|\tilde{0}\rangle$. As neutron p-h interaction, the Sussex matrix elements [42]) have been calculated for the configuration space chosen, i.e., $p \in \{2f_{\frac{7}{2}}, 3p_{\frac{3}{2}}, 1h_{\frac{9}{2}}, 3p_{\frac{1}{2}}, 2f_{\frac{5}{2}}\}$ and $h \in \{2d_{\frac{3}{2}}, 3s_{\frac{1}{2}}, 2d_{\frac{5}{2}}, 1g_{\frac{7}{2}}\}$.

3.2. BASIS FUNCTIONS AND DIAGONALISATION

The problem now is finding the eigenfunctions $|N = 82, Z; I_\alpha M\rangle$ and energy eigenvalues $E_I^{(\alpha)}$ of the Hamiltonian (3.1), with $|N = 82, Z; I_\alpha M\rangle$ expanded in eigenfunctions of the zero-order Hamiltonian $H = H_c + H_p + H_h$, as

$$|N = 82, Z; I_\alpha M\rangle = \sum_{j_h, j_p, N, R, J} f_\alpha(j_h[j_p, NR]_J; I) \times [\tilde{a}_{j_h}(\nu) \otimes [a^+_{j_p}(\nu) \otimes \Omega^+_{NR}]_J]_{IM} |\tilde{0}\rangle. \tag{3.3}$$

The secular equation then becomes

$$\sum_{j_p, j_h, N, R, J} f_\alpha(j_h[j_p, NR]_J; I)\{\langle j_{h'} \otimes [j_{p'} \otimes N'R']_{J'}; IM| H_{p-c}+H_{h-c}+V_{p-h}|j_h \otimes [j_p \otimes NR]_J; IM\rangle + \delta_{j_h j_{h'}}\delta_{j_p j_{p'}}\delta_{NN'}\delta_{RR'}\delta_{JJ'}(\varepsilon_{j_p}+\tilde{\varepsilon}_{j_h}+(N+\tfrac{5}{2})\hbar\omega_2)\} = E_I^{(\alpha)} f_\alpha(j_{h'}[j_{p'}, N'R']_{J'}; I), \tag{3.4}$$

where ε_{j_p} and $\tilde{\varepsilon}_{j_h}$ represent the single-particle and single-hole energies, respectively.

It is now possible to use a representation of particle (hole)-core coupled states, which diagonalises part of the residual interaction in a unified-model description for the $N = 83$, Z ($N = 81$, Z) nuclei. In eq. (2.1), a unified-model description was introduced for the $N = 83$, Z nuclei. The expansion coefficients $c_\beta(j_p, NR; J)$ and the eigenvalues $\omega_J^{(\beta)}$ follow from the equation

$$(H_c+H_{p-c}+H_p)|N=83, Z; J_\beta M\rangle = \omega_J^{(\beta)}|N=83, Z; J_\beta M\rangle. \tag{3.5}$$

With the coefficients $c_\beta(j_p, NR; J)$ thus obtained, one can then construct the GNPH states used as basis vectors in the expansion (2.6) for the $N = 82$, Z nuclei. They are defined by

$$|j_h \otimes J_\beta; IM\rangle \equiv [\tilde{a}_{j_h}(\nu) \otimes |N = 83, Z; J_\beta\rangle]_{IM} = \sum_{j_p, N, R} c_\beta(j_p, NR; J)[\tilde{a}_{j_h}(\nu) \otimes [a^+_{j_p}(\nu) \otimes \Omega^+_{NR}]_J]_{IM}|\tilde{0}\rangle. \tag{3.6}$$

In this basis, part of the residual interaction, i.e., H_{p-c} is diagonal, and the terms $H_{h-c}+V_{p-h}$ remain to be diagonalized for a description of the negative-parity levels in the doubly even $N = 82$ nuclei. Expanding as in eq. (2.6) in the new set of basis wave functions, one obtains for the coefficients d_α, the secular equation

$$\sum_{j_h, J, \beta} d_\alpha(j_h, J_\beta; I)\{\langle j_{h'} \otimes J'_{\beta'}; IM|H_{h-c}+V_{p-h}|\, j_h \otimes J_\beta; IM\rangle + \delta_{j_h j_{h'}}\delta_{JJ'}\delta_{\beta\beta'}(\omega_J^{(\beta)}+\tilde{\varepsilon}_{j_h})\} = E_I^{(\alpha)} d_\alpha(j_{h'}, J'_{\beta'}; I). \tag{3.7}$$

A relation between the coefficients c_β, d_α and f_α exists

$$f_\alpha(j_h[j_p, NR]_J; I) = \sum_\beta d_\alpha(j_h, J_\beta; I) c_\beta(j_p, NR; J). \tag{3.8}$$

The non-diagonal matrix elements can be reduced further as

$$\langle j_{h'} \otimes J'_{\beta'}; IM|H_{h-c}+V_{p-h}|j_h \otimes J_\beta; IM\rangle = \sum_{\substack{j_p, N, R, J_1 \\ j_{p'}, N', R'}} \{(2J+1)(2J'+1)\}^{\frac{1}{2}}(2J_1+1)(-1)^{j_p+j_{p'}+j_h+j_{h'}} \times c_\beta(j_p, NR; J) c_{\beta'}(j_{p'}, N'R'; J') \left\{(-1)^{J+J'} \begin{Bmatrix} I & j_p & J_1 \\ R & j_h & J \end{Bmatrix}\right.$$

$$\times \begin{Bmatrix} I & j_{p'} & J_1 \\ R' & j_{h'} & J' \end{Bmatrix} \delta_{j_p j_{p'}} 0.5\xi_2 \hbar\omega_2 (-1)^{J_1+\frac{1}{2}} \{(2j_h+1)(2j_{h'}+1)\}^{\frac{1}{2}}$$

$$\times \begin{Bmatrix} j_h & R & J_1 \\ R' & j_{h'} & 2 \end{Bmatrix} \begin{pmatrix} j_{h'} & 2 & j_h \\ -\frac{1}{2} & 0 & \frac{1}{2} \end{pmatrix} [(-1)^R \langle NR||b_2^+||N'R'\rangle + (-1)^{R'}$$

$$\times \langle N'R'||b_2^+||NR\rangle] \delta_{\text{even}}^{l+l'} - \delta_{NN'}\delta_{RR'} \begin{Bmatrix} I & R & J_1 \\ j_p & j_h & J \end{Bmatrix} \begin{Bmatrix} I & R' & J_1 \\ j_{p'} & j_{h'} & J' \end{Bmatrix}$$

$$\times \sum_{J''} (2J''+1) \begin{Bmatrix} j_h & j_p & J_1 \\ j_{h'} & j_{p'} & J'' \end{Bmatrix} \langle j_h j_p; J''|V_{p-h}|j_{h'} j_{p'}; J''\rangle \Bigg\}. \tag{3.9}$$

The numerical values of the required boson c.f.p. $\langle NR||b_2^+||N'R'\rangle$ are given in ref. [43]).

The first part of the interaction matrix element contains the contribution from the hole-core coupling and the second part of the residual particle-hole interaction. The $2f_{\frac{7}{2}}$, $2f_{\frac{5}{2}}$, $3p_{\frac{3}{2}}$, $3p_{\frac{1}{2}}$, $1h_{\frac{9}{2}}$ orbits are taken as neutron-particle states and the $3s_{\frac{1}{2}}$, $2d_{\frac{3}{2}}$, $2d_{\frac{5}{2}}$, $1g_{\frac{7}{2}}$ orbits as neutron-hole states. Up to three quadrupole phonons are taken into account. The value of the lowest GNPH energy (cf. eq. (3.7)) is equal to $\omega_{\frac{7}{2}}^{(1)} + \tilde{\varepsilon}_{2d\frac{3}{2}}$ for all doubly even $N = 82$, Z nuclei and was taken as $B_n(N = 82, Z) - B_n(N = 83, Z)$, where $B_n(N, Z)$ denotes the neutron separation energy in the nucleus (N, Z). These values can be obtained from the mass tables of Wapstra and Gove [44]).

3.3. PARAMETERS

In order to evaluate better the agreement between theory and experiment, we are going to discuss the underlying parameters of the model i.e. particle-core and hole-core coupling strength as well as the unperturbed energies ω_{J_β} and $\tilde{\varepsilon}_{j_h}$ used. The bare particle (hole)-vibrational coupling strength can be given as [2, 45, 46])

$$\xi_2 = \left\langle r \frac{\partial V}{\partial r} \right\rangle \frac{4}{\hbar\omega} \frac{(5\pi)^{\frac{1}{2}}}{3Z_e R_0^2} B(\text{E2}; 2^+ \to 0^+)^{\frac{1}{2}}. \tag{3.10}$$

The radial matrix element is estimated to be $\langle r\partial V/\partial r\rangle \approx 50$ MeV [refs. [1, 47])] or can also be calculated by means of a Woods-Saxon average potential to be of the same order of magnitude [48]). The transition probabilities can be deduced from the underlying core vibrational motion (doubly even $N = 82$ nuclei).

Another, equivalent expression † for the coupling strength is

$$\xi_2 = \left\langle r \frac{\partial V}{\partial r} \right\rangle \beta_2 \frac{(\pi)^{-\frac{1}{2}}}{\hbar\omega}, \tag{3.11}$$

with β_2, the rms deformation parameter in the vibrational motion ($\beta_2 = (5\hbar\omega/2C)^{\frac{1}{2}}$),

† Eq. (3.11) leads to a coupling strength for the particle-vibration coupling $\langle r\partial V/\partial r\rangle\beta_\lambda/(2\lambda+1)$, which is consistent with the coupling strength, defined as $\Lambda_\lambda(t_z)$ in ref. [49]), up to two small differences: (i) the $\langle r^\lambda\rangle$ normalization, which however is compensated for by the form factor r^λ occurring within the single-particle part of the interaction ($r^\lambda Y_{\lambda\mu}$) as used in ref. [49]); (ii) the isospin dependence $1+2t_z(N-Z)/A$, which is further discussed in ref. [49]).

TABLE 3

Estimates for the coupling strength ξ_2 in the $N = 83$ and $N = 81$ nuclei by using eqs. (3.10) and (3.11) (indicated by theory I and theory II, respectively)

	^{136}Xe	^{138}Ba	^{140}Ce	^{142}Nd	^{144}Sm
$N = 83$	1.30	1.40	1.50	1.40	1.20
$N = 81$	1.20	1.20	1.20	1.20	1.10
Theory I		2.3±0.7 [b])	1.97±0.3 [b])	2.05±0.25 [b])	1.45±0.25 [f])
Theory II	1.26 [a])	1.35 [c])	1.31 [d])	1.7±0.3 [e])	1.20 [g])

A comparison with the best fit values for these nuclei is given in the first and second row.
[a]) Ref. [50]). [b]) Ref. [51]). [c]) Ref. [52]). [d]) Ref. [53]). [e]) Ref. [54]). [f]) Ref. [55]).
[g]) Ref. [56]).

as can be determined directly in (p, p′) or (α, α′) inelastic scattering experiments.

Effects of residual interactions [49]), neglected in this approach, can be included in a renormalization of the bare coupling strength thus obtained. As no large renormalization effects are expected [49]), we have fitted ξ_2 in order to obtain as good agreement as possible in the $N = 83$ and $N = 81$ nuclei. As one can see in table 3, the best fit values for ξ_2 agree very well with the theoretical estimate. For the unperturbed energies ω_{J_β}, the experimental excitation energies of known levels in the $N = 83$ nuclei with $E_x \lesssim 2.0$ MeV and definite J^π values are used, as indicated in fig. 1,

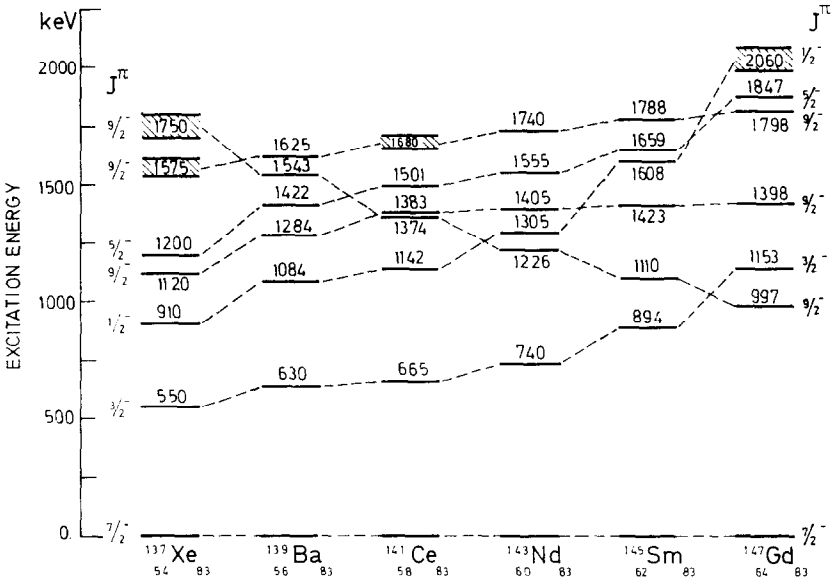

Fig. 1. The experimental excitation energies for the low-lying levels in the $N = 83, Z$ nuclei with definite J_β^π assignments, for ^{137}Xe up to ^{147}Gd. The shaded regions are obtained by extrapolating.

whereas for $\tilde{\varepsilon}_{jh}$, the centroid values [57]) for the different neutron-hole states as measured in neutron pick-up reactions by Jolly and Kashy, are used.

3.4. TRUNCATION EFFECTS

As the $J^\pi = \frac{3}{2}^+$ ground state and the $J^\pi = \frac{1}{2}^+$ first excited state in all $N = 81$, Z nuclei are almost pure single-neutron hole states, as follows from the spectroscopic factors [33]), one might wonder whether the residual hole-core interaction would not be much smaller than the neutron hole-particle interaction. In order to study these effects, we have diagonalized in the basis of GNPH states, the residual interaction $H_{h-c}+V_{p-h}$ in two different two-step processes:

(i) First a diagonalization of H_{h-c} is performed and in the obtained new basis V_{p-h} is diagonalized afterwards.

(ii) First a diagonalization of V_{p-h} and afterwards, in the new basis, a diagonalization of H_{h-c} is performed.

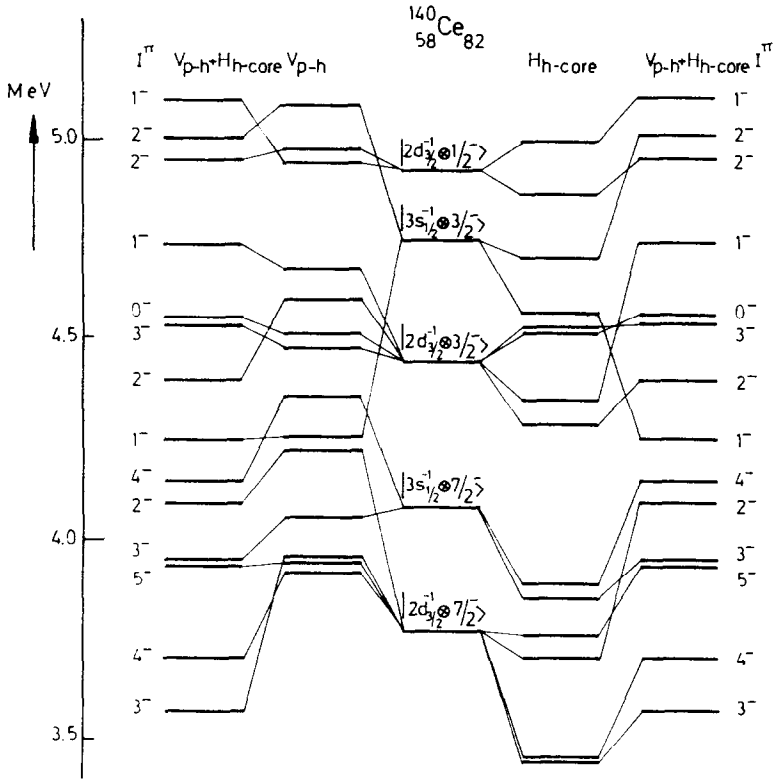

Fig. 2. Diagonalization results for ^{140}Ce for the lower negative-parity neutron particle-hole states. The spectra labeled V_{p-h} and H_{h-c} result from diagonalizing only these two parts of the residual interaction, while the column $V_{p-h}+H_{h-c}$ represents the spectrum for the complete residual interaction.

The results, in the case of ^{140}Ce, are shown in fig. 2, for the $|2d_{\frac{5}{2}}^{-1} \otimes 7^-_{2(1)}\rangle$, $|3s_{\frac{1}{2}}^{-1} \otimes 7^-_{2(1)}\rangle$, $|2d_{\frac{5}{2}}^{-1} \otimes 3^-_{2(1)}\rangle$, $|3s_{\frac{1}{2}}^{-1} \otimes 3^-_{2(1)}\rangle$ and $|2d_{\frac{5}{2}}^{-1} \otimes 1^-_{2(1)}\rangle$ multiplets. One observes that diagonalization of V_{p-h} already contains the most important contribution from the residual interaction and mainly results in a shift to higher excitation energies. The approximation of neglecting H_{h-c} as made by Wurm *et al.* [22]), is a reasonable first approximation, but in order to obtain a more quantitative description, both parts of the residual interaction should be taken into account.

4. Level schemes, partial decay widths, angular distributions and spectroscopic factors for the doubly even $N = 82$ nuclei

For all $N = 82$ nuclei, in figs. 6, 8, 10, 13, 14 and 16, the theoretical level schemes are given and compared to the experimental data on energy and feeding through the IAR. Also, the positive-parity levels, calculated in a two quasi-particle (2QP) calculation [37]), as well as collective levels, obtained from coupling the one-quadrupole and one-octupole vibrational states [58]) are given. In cases where the spectroscopic factors are available ($S_{p,p}$ or $S_{d,p}$), these data are extensively discussed and compared with the theoretical results.

Although separate groups of levels are fed through the $7^-_{2(1)}$ and $3^-_{2(1)}$ IAR, a better test on the structure of the final, negative-parity levels in the doubly even $N = 82$ isotones is offered by a calculation of partial decay widths and the systematic changes of the widths for inelastic proton scattering through the lowest two IAR states (figs. 3 and 4).

For both the $7^-_{2(1)}$ and $3^-_{2(1)}$ resonances, the partial decay widths are stable in going from ^{136}Xe to ^{142}Nd, when placed relative to the experimental $I^\pi = 4^-$ lowest level with definite neutron particle-hole nature (in the theoretical calculation, the lowest $I^\pi = 3^-$ level is taken as reference level). The partial decay width to the $I^\pi = 4^-_{(1)}$ level is always reproduced with too small a value, whereas the widths to the other levels $I^\pi_\alpha = 2^-_{(1)}$, $3^-_{(1)}$, $3^-_{(2)}$, $4^-_{(2)}$ and $5^-_{(1)}$ are reproduced very well. Via the $3^-_{2(1)}$ resonance, the $I^\pi_\alpha = 1^-_{(1)}$ and $2^-_{(2)}$ levels are fed dominantly, as well theoretically as experimentally. Here, unique assignments cannot be made, although the overall distribution of inelastic proton strength is reproduced fairly good.

By using formulae (2.9)–(2.12), it is also possible, with the knowledge of the wave functions, to calculate angular distributions. In fig. 5 the systematics of angular distributions through the $7^-_{2(1)}$ IAR is shown for all doubly even $N = 82$ isotones. There is good agreement in general, although for the $I^\pi_\alpha = 3^-_{(1)}$ level, there is more structure in the experimental results, whereas the $I^\pi_\alpha = 3^-_{(2)}$ calculated distribution curves in the opposite direction as compared to the experiment.

The general overall agreement of the calculated partial decay widths and angular distributions through the $7^-_{2(1)}$ IAR, and the calculated level schemes with experiment, clearly show the occurrence of rather pure GNPH states in all doubly even $N = 82$ isotones for $I^\pi_\alpha = 4^-_{(1)}$, $4^-_{(2)}$, $5^-_{(1)}$.

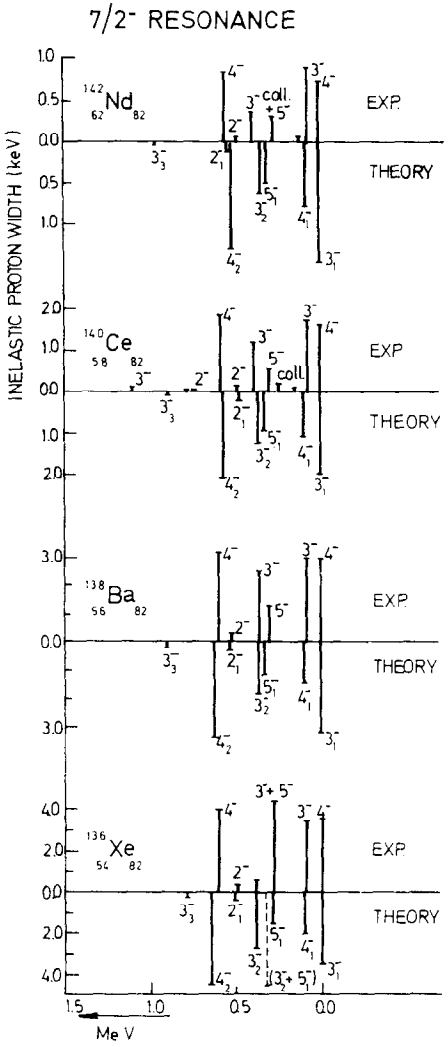

Fig. 3. Experimental and theoretical partial decay-width systematics on the $\frac{7}{2(1)}^-$ state.

The levels $I^\pi_\alpha = 3^-_{(1)}$, $3^-_{(2)}$ and $2^-_{(1)}$ however, are strongly mixed states built from the $|2d^{-1}_{\frac{3}{2}} \otimes \frac{7}{2(1)}^-\rangle$, $|3s^{-1}_{\frac{1}{2}} \otimes \frac{7}{2(1)}^-\rangle$ and $|2d^{-1}_{\frac{3}{2}} \otimes \frac{3}{2(1)}^-\rangle$ GNPH configurations.

The angular distributions for the $\frac{3}{2(1)}^-$ IAR are more diversified and special attention has been given in comparing experimental data and theoretical results.

The nucleus ^{136}Xe. The levels with $E_x \lesssim 5.0$ MeV, excited through the $\frac{7}{2(1)}^-$, $\frac{3}{2(1)}^-$ and $\frac{1}{2(1)}^-$ IAR are compared with the theoretical calculations in fig. 6. The reversed order, as obtained from the lowest $I^\pi_\alpha = 3^-_{(1)}$ and $4^-_{(1)}$ levels, is characteristic for all other doubly even $N = 82$ nuclei, when compared to the experimental situation.

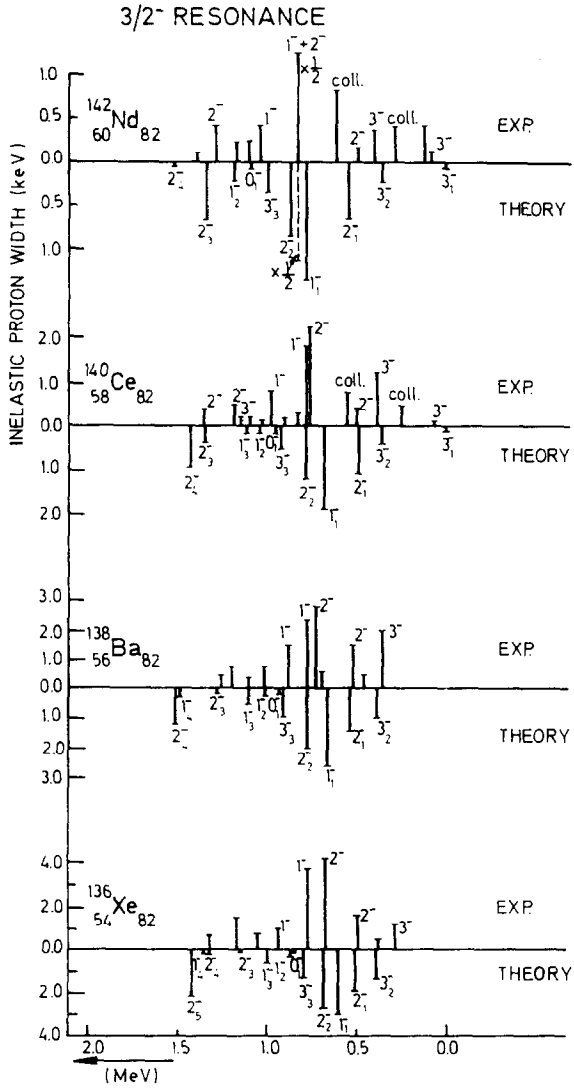

Fig. 4. Experimental and theoretical partial decay-width systematics on the $\frac{3}{2}^-_{(1)}$ IAR state.

The $I^\pi = 1^-, 2^-$ doublet, strongly excited through the $\frac{3}{2}^-_{(1)}$ IAR in all doubly even $N = 82$ isotones is reproduced rather well theoretically. This concerns the excitation energy, the partial decay widths, as well as the angular distribution (fig. 7). The experimental $I^\pi = 2^-$ assignment to a level at 4.71 MeV is shown to agree best with the $I^\pi_\alpha = 1^-_{(3)}$ calculated level, a fact which is also shown in the partial decay-width calculation (fig. 4). This suggestion was also made some time ago by the Heidelberg group. From eq. (2.4) and the measured proton partial decay widths [19, 20]), spectroscopic factors $S_{p,p}$ can be obtained and are compared with the theoretical results

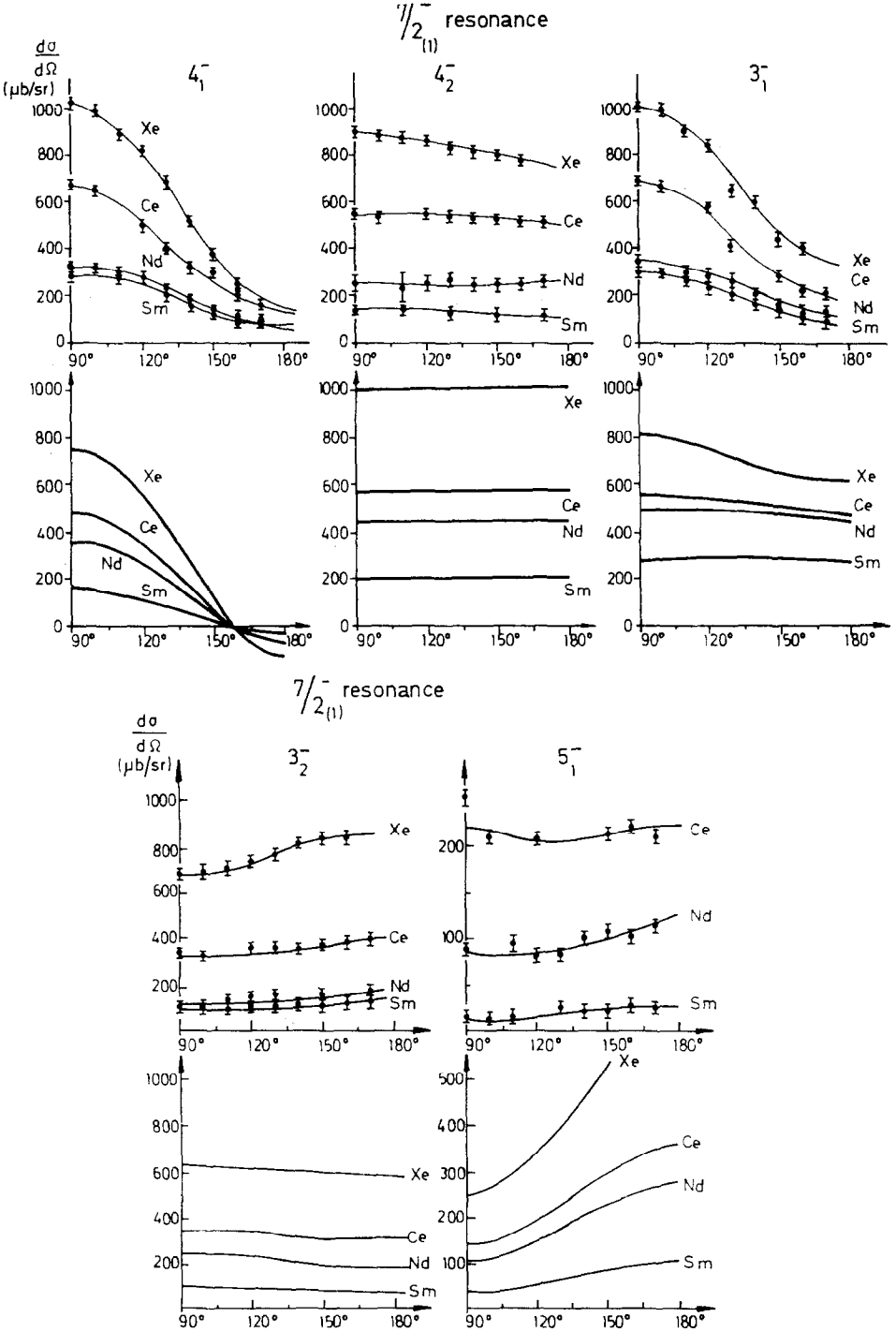

Fig. 5. Angular distributions $d\sigma/d\Omega$ (μb/sr), in their systematic behaviour on the $\frac{7}{2}_{(1)}^-$ IAR for the $I_\alpha^\pi = 4_{(1)}^-$, $4_{(2)}^-$, $3_{(1)}^-$, $3_{(2)}^-$ and $5_{(1)}^-$ levels. For ^{136}Xe, ref. [20]) is used; for ^{140}Ce, ^{142}Nd, the Heidelberg data are used and for ^{144}Sm, the Montreal data are used, in order to make a comparison with the theoretical results.

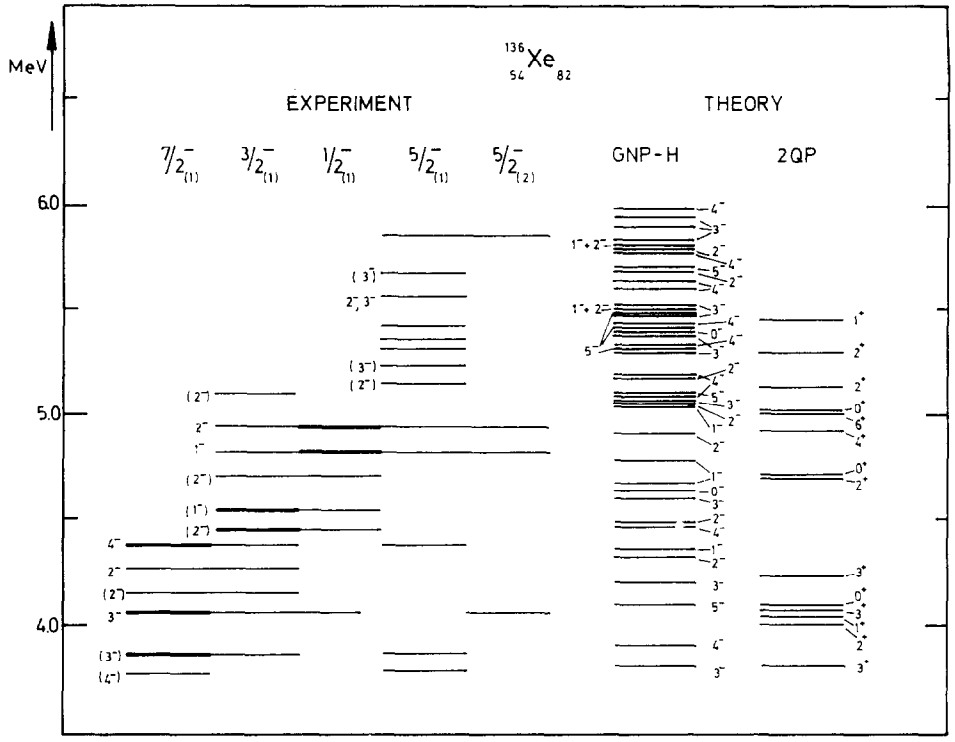

Fig. 6. Comparison of experimental data and theoretical calculation. Each column of experimental levels is headed by the IAR through which they are mainly fed. The theoretical spectra result from (i) GNPH calculation; (ii) 2QP calculation [37]); (iii) collective, negative-parity levels [58]).

TABLE 4

Spectroscopic factors $S_{p,p'}$ ($3s_{\frac{1}{2}}$) and $S_{p,p'}$ ($2d_{\frac{3}{2}}$) for negative-parity levels in ^{136}Xe compared to the theoretical values

E_x (MeV)	I^π	$S_{p,p'}$ ($3s_{\frac{1}{2}}$)		$S_{p,p'}$ ($2d_{\frac{3}{2}}$)	
		exp. [a])	th.	exp. [a])	th.
3.26	$\underline{3}^-$, (5^-)	0.07		0.03	
3.78	$\underline{3}^-$, $\underline{4}^-$	0.08	0.01	0.87	0.92
3.87	$\underline{3}^-$, $\underline{4}^-$	0.24	0.33	0.81	0.51
4.06	$\underline{3}^-$	0.48	0.40	0.07	0.94
4.27	$\underline{2}^-$	0.06		0.21	0.75
4.38	(3^-), $\underline{4}^-$	0.64	0.86	0.05	0.02
4.45	$\underline{1}^-$, $\underline{2}^-$	0.29	0.05	0.21	0.86
4.54	$\underline{1}^-$, $\underline{2}^-$	0.51	0.42	0.13	0.08
4.71	$\underline{2}^-$	0.07	0.01	0.06	0.04
4.82	$\underline{1}^-$			0.66	0.62

The onderlined spin values are used in extracting spectroscopic factors.
[a]) Refs. [18, 19]).

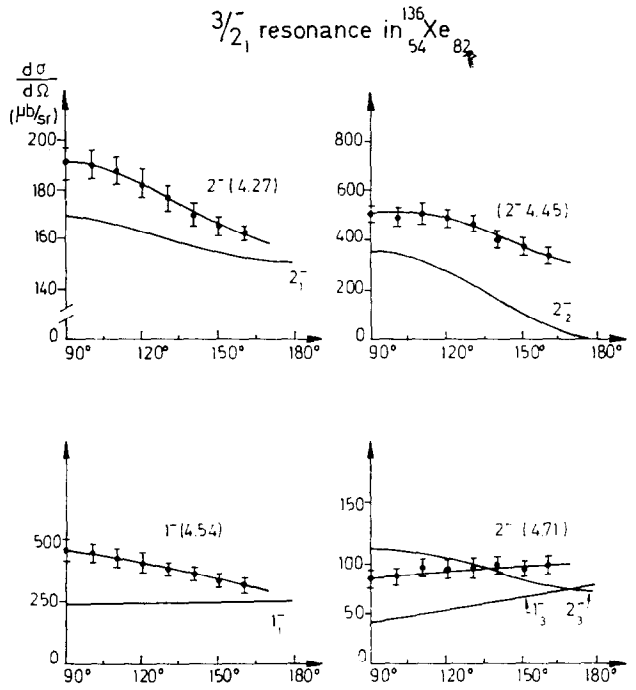

Fig. 7. Angular distributions for ^{136}Xe on the $\frac{3}{2}^-_{(1)}$ IAR. The heavy full line indicates the theoretical result. Experimental data points [20]) and the experimental fit, using eq. (2.9), are also indicated.

in table 4. Generally, there is good agreement. For the higher-lying levels, mainly fed through the $\frac{5}{2}^-_{(1),(2)}$ IAR, no unique assignments could be made.

The nucleus ^{138}*Ba.* In the case of ^{138}Ba, levels are fed through the $\frac{7}{2}^-_{(1)}$, $\frac{3}{2}^-_{(1)}$ and $\frac{1}{2}^-_{(1)}$ IAR. These are shown in fig. 8. In this case, the reaction ^{137}Ba(d, p)^{138}Ba indicates [21]) the possibility of direct feeding from the $J^\pi = \frac{3}{2}^+$ ground state of ^{137}Ba (mainly a $2d^{-1}_{\frac{3}{2}}$ neutron-hole state) to GNPH configurations in the final, negative-parity levels $|2d^{-1}_{\frac{3}{2}} \otimes J_\beta; I^-\rangle$. In the transfer reactions, a $l_n = 1$ and $l_n = 3$ transfer is clearly observed to levels in the energy region 3.5 MeV $\lesssim E_x \lesssim$ 6.0 MeV that are also fed in the proton decay of the $\frac{7}{2}^-_{(1)}$, $\frac{3}{2}^-_{(1)}$ and $\frac{1}{2}^-_{(1)}$ IAR. The measured spectroscopic factor for l_j transfer in a neutron stripping reaction from the $\frac{3}{2}^+_{(1)}$ ground state in ^{137}Ba is calculated as

$$S^{(\alpha)}_{lj}(\tfrac{3}{2}^+_{(1)}) = |\langle N = 82, Z; I_\alpha M|[a^+_{lj}(\nu) \otimes |N = 81, Z; \tfrac{3}{2}^+_{(1)}\rangle]; IM|^2, \qquad (4.1)$$

or more explicitly

$$S^{(\alpha)}_{lj}(\tfrac{3}{2}^+_{(1)}) = |\sum_{j_h, N, R, J'} k_1(j_h, NR; \tfrac{3}{2}^+) f_\alpha(j_h[j, NR]_{J'}; I) \times 2(2J'+1)^{\frac{1}{2}} W(jJ'\tfrac{3}{2} j_h; RI)|^2. \qquad (4.2)$$

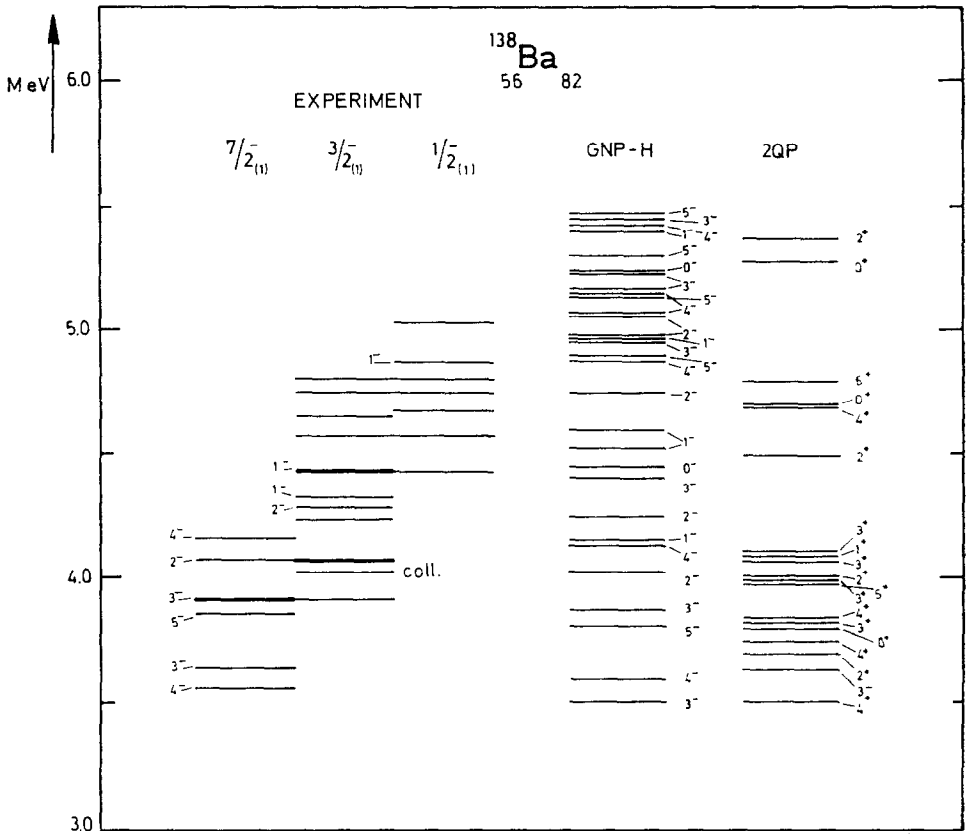

Fig. 8. See caption to fig. 6.

The expansion amplitudes $k_1(j_h, NR; \frac{3}{2}^+)$ and $f_\alpha(j_h[j_p, NR]\,J'; I)$, defined in eq. (3.8), describe the $N = 81$, Z and $N = 82$, Z nuclei, respectively.

If the $\frac{3}{2}^+$ ground state is mainly considered as a pure $2d_{\frac{3}{2}}^{-1}$ neutron-hole state, eq. (4.2) reduces to

$$S_{ij}^{(\alpha)}(\tfrac{3}{2}^+_{(1)}) = |\sum_\beta d_\alpha(2d_{\frac{3}{2}}, J_\beta; I) c_\beta(J, 00, J)|^2. \tag{4.3}$$

In fig. 9, these spectroscopic factors are compared to the experimental data [21]) and show good agreement. This comparison clearly indicates the neutron particle-hole nature of the higher-lying negative-parity levels.

The nucleus ^{140}Ce. It can be shown that most negative-parity levels below $E_x \approx 5.0$ MeV can be understood in terms of a coupling between GNPH states, built on the lowest $J^\pi = \frac{7}{2}^-, \frac{3}{2}^-$ and $\frac{1}{2}^-$ $N = 83$ levels, as shown in fig. 10.

In table 5, wave functions for the lowest three $I^\pi = 3^-$ and lowest two $I^\pi = 4^-$ levels are compared with experimental data [22]) and show good agreement both for the magnitudes and the relative signs. The $I_\alpha^\pi = 5^-_{(1)}$ level observed is an almost pure

TABLE 5

Amplitudes of the experimental and theoretical wave functions for the lowest three $I^\pi = 3^-$ and lowest two $I^\pi = 4^-$ levels

I_α^π	3_1^-		3_2^-		3_3^-		4_1^-		4_2^-	
$\lvert d_{\frac{3}{2}}^{-1} \otimes 2_1^+ \rangle$	0.784 23	0.69	0.27 4	0.62	0.25 15	0.23	0.927 5	0.963	−0.374 5	−0.071
$\lvert s_{\frac{1}{2}}^{-1} \otimes 2_1^+ \rangle$	−0.553 7	−0.62	0.688 5	0.64	0.45 5	0.21	0.365 5	0.06	0.896 5	0.939
$\lvert d_{\frac{3}{2}}^{-1} \otimes 0_1^+ \rangle$	−0.24 8	0.06	−0.653 16	0.38	0.5 2	−0.85				
$\lvert d_{\frac{3}{2}}^{-1} \otimes 4_1^+ \rangle$	< 0.15	0.11	< 0.15	0.10	< 0.5	0.26	< 0.15	−0.12	< 0.15	−0.04
$\lvert d_{\frac{5}{2}}^{-1} \otimes 2_1^+ \rangle$	−0.12 2	0.15	0.02 4	0.02	0.45 10	0.17	0.08 2	0.08	0.24 2	0.075
$\lvert d_{\frac{5}{2}}^{-1} \otimes 0_1^+ \rangle$	−0.08 13	−0.01	−0.17 2		0.3 2	0.09	< 0.15	0.03	< 0.15	−0.11

Only the most important GNPH configurations are given. The experimental values are given at the left (experimental error in the second row) and theoretical values at the right.

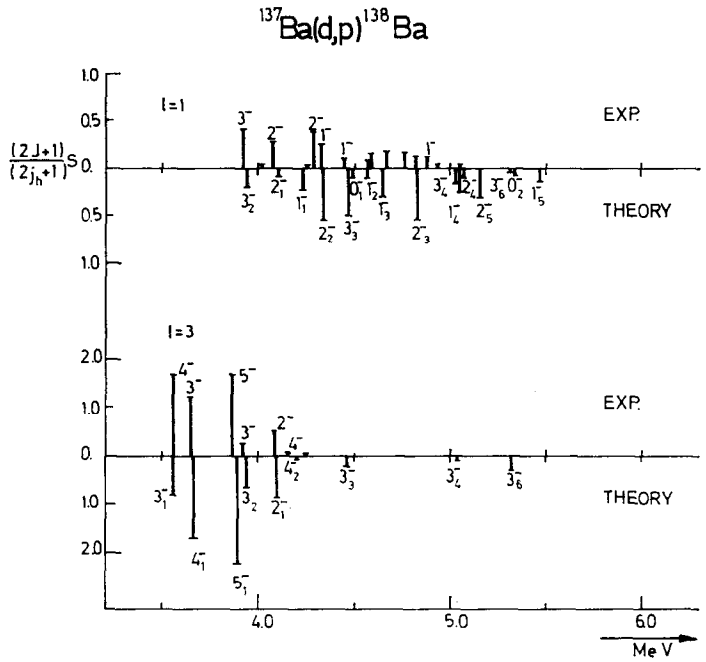

Fig. 9. The spectroscopic factor $S(2J+1)/(2j_h+1)$ for neutron stripping from ^{137}Ba to negative-parity levels I_α in the final doubly even ^{138}Ba nucleus (for $l_n = 1$ and $l_n = 3$) as compared to the theoretical values.

$|2d_{\frac{3}{2}}^{-1} \otimes 7^-_{2(1)}\rangle$ GNPH state, which is confirmed by the selective feeding of this level through the $7^-_{2(1)}$ IAR. The lowest $I^\pi_\alpha = 2^-_{(1)}$ level contains the $|2d_{\frac{3}{2}}^{-1} \otimes 7^-_{2(1)}\rangle$ GNPH state with an amplitude of 0.85 whereas the $|3s_{\frac{1}{2}}^{-1} \otimes 3^-_{2(1)}\rangle$ GNPH state occurs with an amplitude of -0.37. The penetrability of the s-wave proton is strongly enhanced over d-wave proton emission, resulting in a stronger feeding of this $I^\pi_\alpha = 2^-_{(1)}$ level through the $3^-_{2(1)}$ IAR, a fact which is also observed experimentally [24, 28]). As is also shown in fig. 11, the theoretical angular distribution through the $3^-_{2(1)}$ IAR towards the $I^\pi_\alpha = 2^-_{(1)}$ level is in good agreement with experimental data. The $I^\pi_\alpha = 2^-_{(2)}$ level is mainly the $|2d_{\frac{3}{2}}^{-1} \otimes 3^-_{2(1)}\rangle$ configuration, whereas the close-lying $I^\pi_\alpha = 1^-_{(1)}$ level mainly consists of the $|3s_{\frac{1}{2}}^{-1} \otimes 3^-_{2(1)}\rangle$ configuration with small admixtures of the $|2d_{\frac{3}{2}}^{-1} \otimes 3^-_{2(1)}\rangle$, $|2d_{\frac{3}{2}}^{-1} \otimes 1^-_{2(1)}\rangle$ and $|3s_{\frac{1}{2}}^{-1} \otimes 1^-_{2(1)}\rangle$ configurations. These results also agree with the very strong feeding of the close-lying $I^\pi_\alpha = 1^-_{(1)}$ and $2^-_{(2)}$ levels through the $3^-_{2(1)}$ IAR.

This doublet, not resolved in the experimental angular distribution (fig. 11) is reproduced very well in the theoretical calculation. The assignment of theoretical values to experimentally observed levels becomes more difficult to establish for the higher-lying states ($E_x \gtrapprox 4.5$ MeV), but is still possible in some cases by considering results obtained from angular distributions.

At $E_x = 4.34$ MeV, and $I^\pi = 1^-$ level is observed, strongly excited through the $3^-_{2(1)}$ IAR, which can be interpreted as the theoretical $I^\pi_\alpha = 1^-_{(3)}$ level, which is mainly

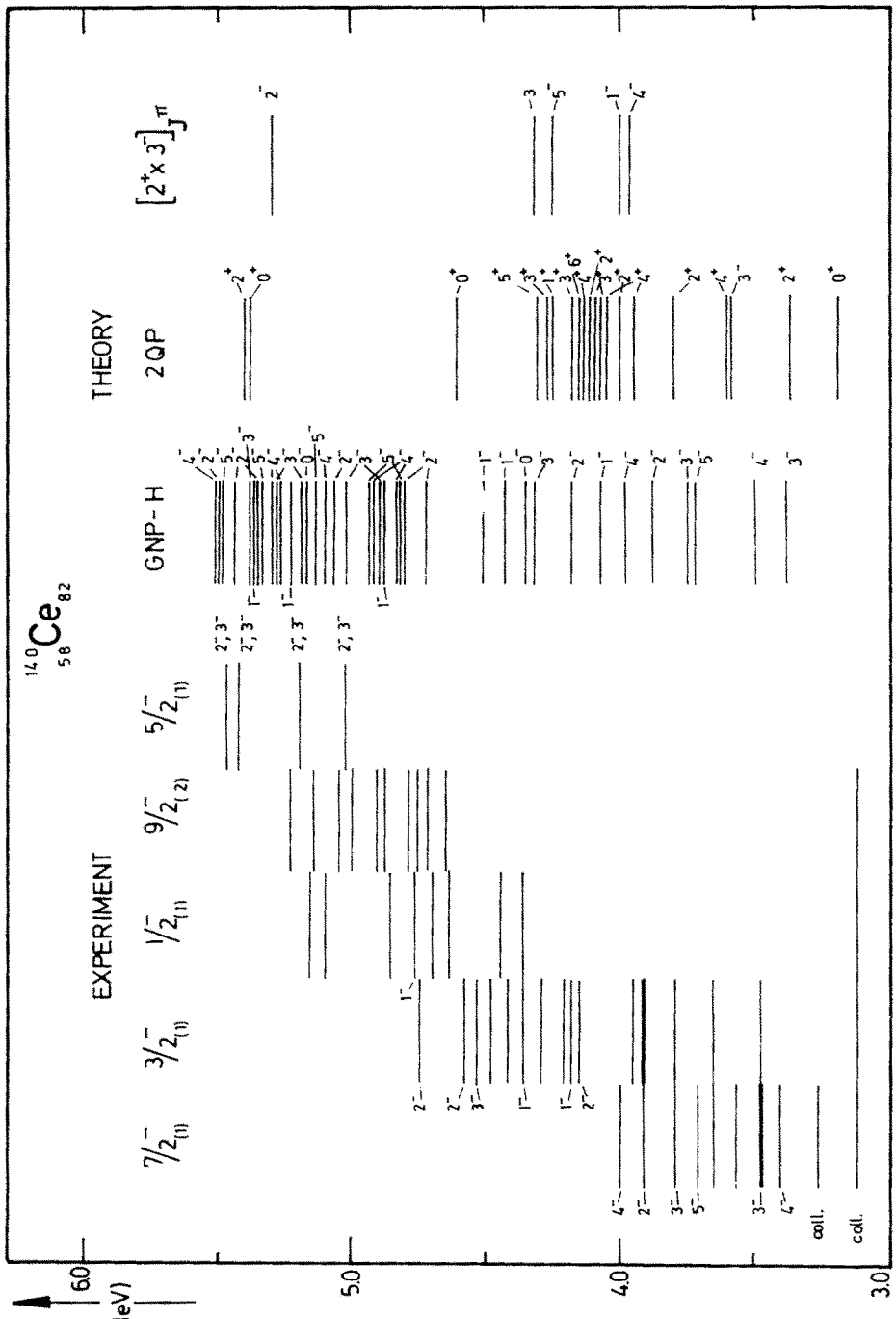

Fig. 10. See caption to fig. 6.

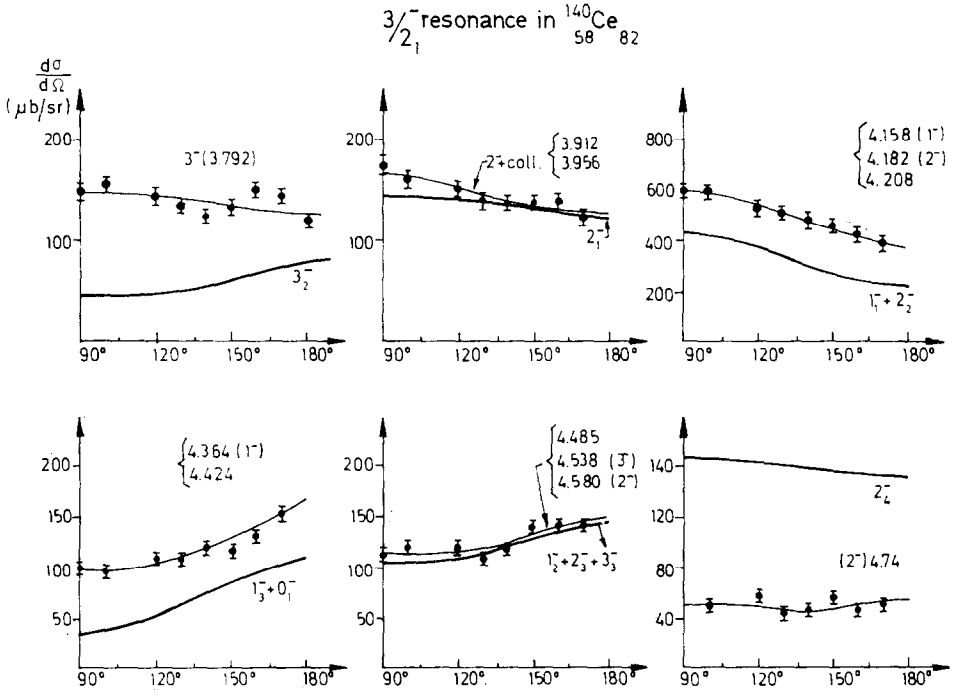

Fig. 11. Same caption as fig. 7, but for ^{140}Ce.

a $|2d_{\frac{3}{2}}^{-1} \otimes 2^{-}_{(1)}\rangle$ GNPH state (amplitude -0.85), with a big admixture of the $|2d_{\frac{3}{2}}^{-1} \otimes 1^{-}_{(1)}\rangle$ configuration (amplitude -0.46). In the angular distribution measurements, at the relevant excitation energy, good agreement is obtained when the $I^{\pi}_{\alpha} = 1^{-}_{(3)}$ and the $0^{-}_{(1)}$ levels are taken into account. At still higher excitation energies, a group of levels (4.485 MeV, 4.538 MeV (3^-) and 4.580 MeV (2^-)) is shown to agree with the theoretical angular distribution as obtained from the $I^{\pi}_{\alpha} = 1^{-}_{(2)} + 2^{-}_{(3)} + 3^{-}_{(3)}$ levels. For the lowes three $I^{\pi} = 2^-$ states, one finds that up to $E_x = 4.6$ MeV, 50 % of the total $|3s_{\frac{1}{2}}^{-1} \otimes 2^{-}_{(1)}; 2^-\rangle$ strength is missing; therefore an $I^{\pi} = 2^-$ state at $E_x = 4.748$ MeV is assigned with a large $|3s_{\frac{1}{2}}^{-1} \otimes 2^{-}_{(1)}\rangle$ component, a fact also confirmed in the theoretical calculation where a $I^{\pi}_{\alpha} = 2^{-}_{(4)}$ level at $E_x = 4.82$ MeV with $|3s_{\frac{1}{2}}^{-1} \otimes 2^{-}_{(1)}; 2^-\rangle$ strength of 46 % is reproduced. The angular distribution for the $1^{-}_{(1)}$ IAR, as shown in fig. 12, to a level at 4.34 MeV (1^-) can be explained by the $I^{\pi}_{\alpha} = 1^{-}_{(3)} + 0^{-}_{(1)}$ assignment, whereas the 4.45 MeV, 4.48 MeV doublet, also fed via the $2^{-}_{(1)}$ resonance, can be explained as a superposition of the $I^{\pi}_{\alpha} = 1^{-}_{(2)}$, $2^{-}_{(3)}$ and $3^{-}_{(3)}$ levels. A $I^{\pi} = 1^-$ level, excited at 4.77 MeV, is reproduced in its angular distribution with a wave function consisting of the $|3s_{\frac{1}{2}}^{-1} \otimes 1^{-}_{(1)}\rangle$ (amplitude 0.60) and $|2d_{\frac{3}{2}}^{-1} \otimes 1^{-}_{(1)}\rangle$ (amplitude 0.59) GNPH configurations.

The nucleus ^{142}*Nd.* In the case of ^{142}Nd, it is possible to compare the early Heidelberg data [22–28]), obtained with a resolution of 35–50 keV with the very recent results

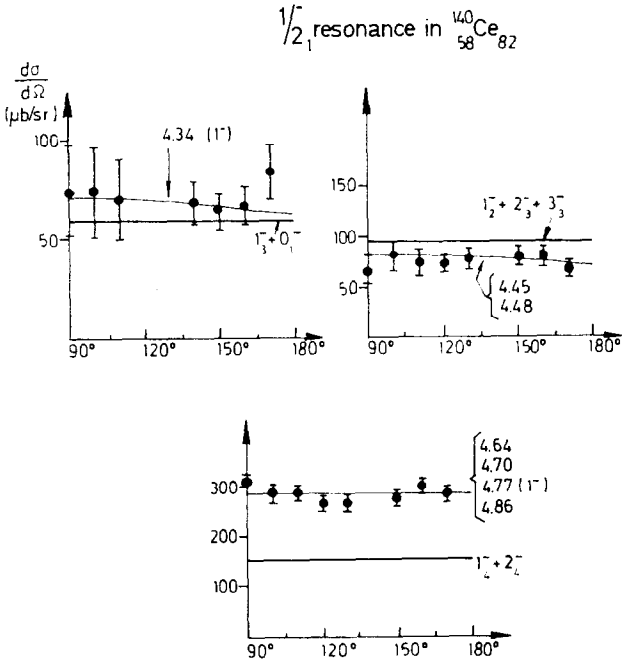

Fig. 12. Same caption as fig. 7; but on the $\frac{1}{2(1)}^-$ IAR for ^{140}Ce.

from the Montreal group [29–32]), measured with a resolution of 15 keV (see fig. 13). There seems to be some disagreement between assignments made by the Montreal group and the Heidelberg group. Taking into account the improved resolution of the former, one can resolve these difficulties (see appendix B). Also, the reaction ^{143}Nd (d, t)^{142}Nd has been performed for $l = 0$ and $l = 2$ neutron pick-up from the $J^\pi = \frac{7}{2}^-$ ^{143}Nd ground state. This leads to final negative-parity levels in ^{142}Nd and again shows clearly the neutron particle-hole nature of these final levels.

The experimental level scheme, as fed through the $\frac{7}{2(1)}^-$ IAR, is compared in fig. 14 with the theoretical negative-parity levels from a GNPH description, with the levels resulting from coupling the quadrupole and octupole vibrational states [58] ($[2^+ \otimes 3^-]$ $I^- = 1^-, 2^-, 3^-, 4^-, 5^-$) and with the relevant unperturbed GNPH configurations. Connections between levels are made on the basis of spectroscopic factors, partial decay widths and angular distribution measurements. Spectroscopic factors for the reaction ^{143}Nd(d, t)^{142}Nd given by the expression

$$S_{lj}^{(\alpha)} = |d_\alpha(lj_p, \tfrac{7}{2(1)}^-; I)|^2, \tag{4.4}$$

are compared in table 6. The larger spectroscopic factors compare well with the theoretical values, although in the case of $I^\pi = 3^-$ and 5^-; the latter are too large. Therefore, in this nucleus, the $I_\alpha^\pi = 3_{(2)}^-$ assignment is difficult to make. There occurs a fragmentation between the $I^\pi = 3^-$ (3.574 MeV) and the $I^\pi = 3^-$ (3.710 MeV)

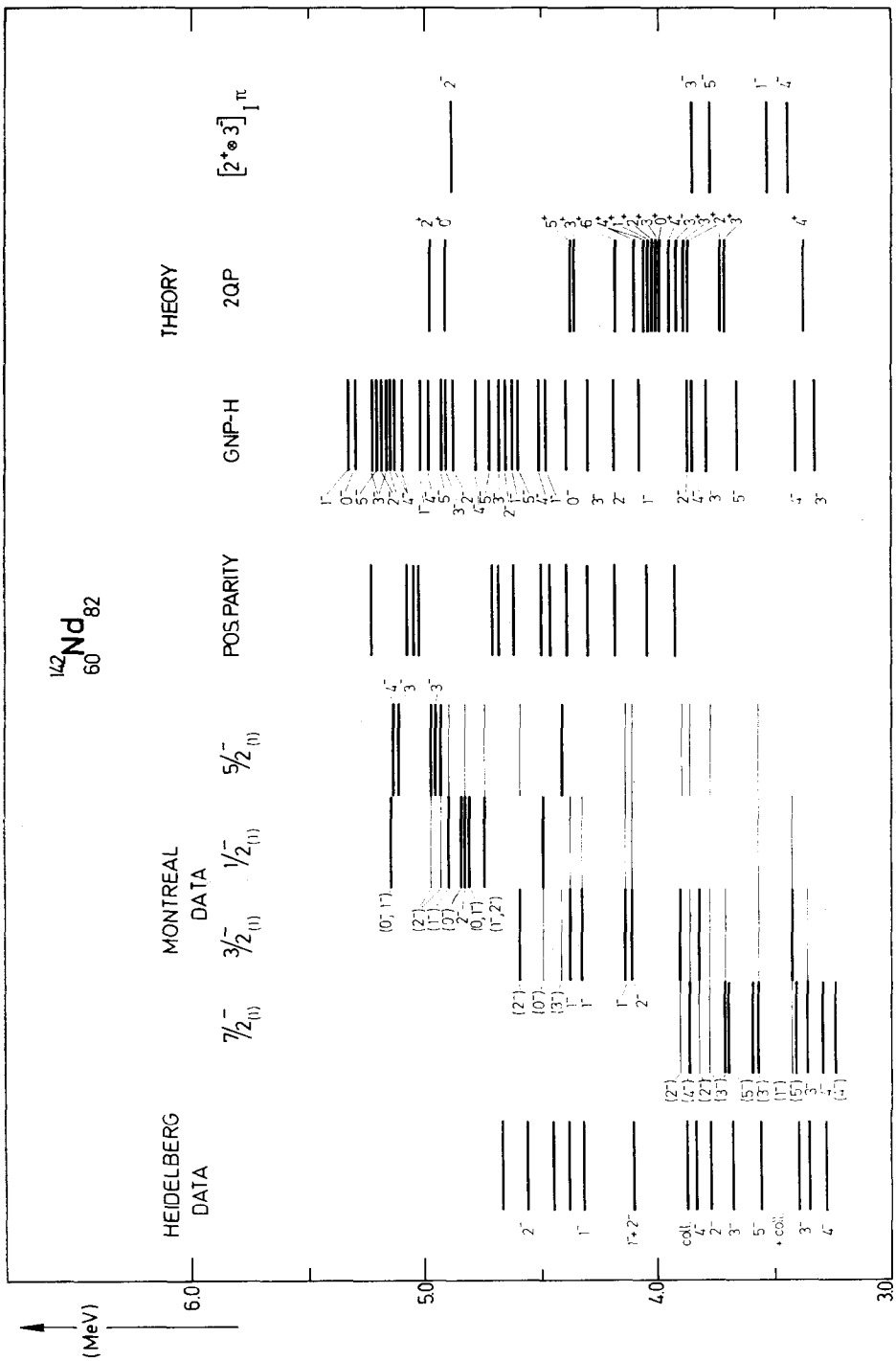

Fig. 13. See caption to fig. 6.

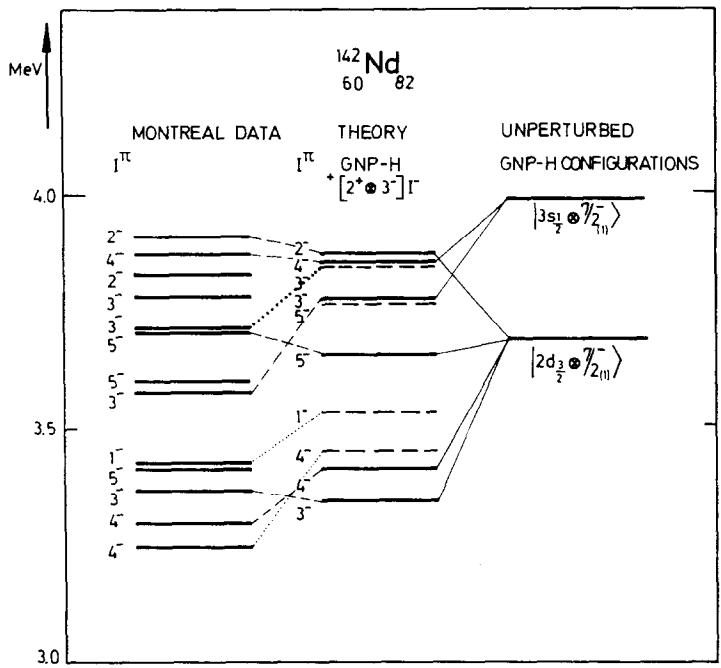

Fig. 14. Levels in ^{142}Nd that are fed strongly through the $\frac{7}{2}_{(1)}^-$ IAR and consist mainly of the GNPH configurations $|3s_{\frac{1}{2}}^{-1} \otimes \frac{7}{2}_{(1)}^-\rangle$ and $|2d_{\frac{3}{2}}^{-1} \otimes \frac{7}{2}_{(1)}^-\rangle$ are compared to the experimental, negative-parity levels.

TABLE 6

Spectroscopic factors for neutron pick-up ($S_{d,t}$ ($3s_{\frac{1}{2}}$) and $S_{d,t}$ ($2d_{\frac{3}{2}}$)) for the levels fed through the $\frac{7}{2}_{(1)}^-$ IAR of ^{143}Nd, and compared to the theoretical values

E_x (MeV)	I^π	$S_{d,t}$ ($s_{\frac{1}{2}}$)		$S_{d,t}$ ($d_{\frac{3}{2}}$)	
		exp. [a])	th.	exp. [a])	th.
3.244	4⁻	0.011±0.005		0.03±0.01	
3.295	4⁻	0.14 ±0.02		0.59±0.04	0.92
3.366	3⁻	0.31 ±0.08	0.47	0.49±0.16	0.37
3.413	5⁻			0.14	
3.574	3⁻	0.15 ±0.01		0.06±0.06	
3.598	5⁻			0.05	
3.705	5⁻			0.46±0.03	0.93
3.710	3⁻	0.13 ±0.01	0.32		0.50
3.779	3⁻	0.015±0.005		0.032±0.01	
3.830	2⁻			0.095	
3.870	4⁻	0.53 ±0.09	0.86	0.18±0.18	0.015
3.908	2⁻			0.26	0.72

[a]) Ref. [31]).

levels, with nearly equal spectroscopic factor $S_{p,p}(3s_{\frac{1}{2}})$, i.e. 0.17 ± 0.01 and 0.16 ± 0.01, respectively. This fact can be explained qualitatively by coupling the $|3s_{\frac{1}{2}}^{-1} \otimes 7_{2(1)}^{-}; 3^- \rangle$ GNPH configuration to the close-lying $[2^+ \otimes 3^-]3^-$ collective level, with a resulting fragmentation of the $|3s_{\frac{1}{2}}^{-1} \otimes 7_{2(1)}^{-}; 3^- \rangle$ strength [59]). The collective states, however, have spectroscopic factors that are smaller by an order of magnitude in comparison to the strong excited neutron particle-hole like, negative-parity levels. The agreement of levels excited through the $\frac{3}{2}^-_{(1)}$ IAR is quite good (fig. 15), as most levels are reproduced theoretically.

Analysis of the levels $I^\pi = 1^-, 2^-$; the splitting of the $|2d_{\frac{3}{2}}^{-1} \otimes \frac{3}{2}^-_{(1)}; I^\pi\rangle$ ($I^\pi = 0^-, 1^-, 2^-, 3^-$) and $|3s_{\frac{1}{2}}^{-1} \otimes \frac{3}{2}^-_{(1)}; I^\pi\rangle$ ($I^\pi = 1^-, 2^-$) levels and the location in excitation energy, can be made due to the better energy resolution as obtained by the Montreal

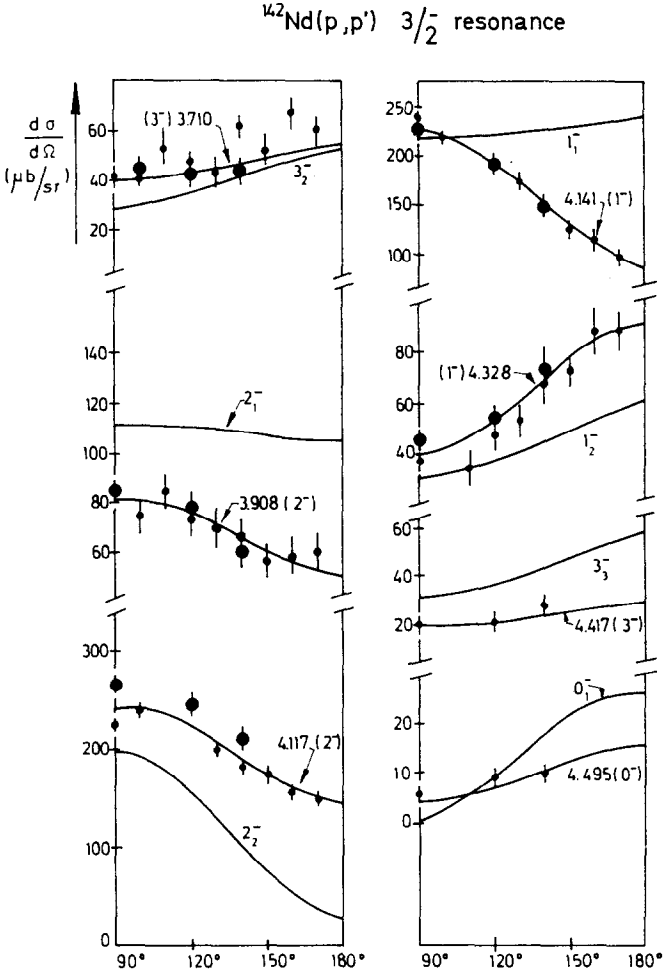

Fig. 15. Same caption as fig. 7; but for ^{142}Nd.

group In the case of ^{142}Nd and ^{144}Sm, the total cross section (mb) has been measured on the $\frac{7}{2}^-_{(1)}$, $\frac{3}{2}^-_{(1)}$, $\frac{1}{2}^-_{(1)}$ and $\frac{5}{2}^-_{(1)}$ isobaric analogue resonances by the Montreal group. These numbers are also calculated and compared with the experimental results in tables 7 and 8. As a general remark, one finds that levels strongly excited experimentally on the IAR, are also strongly fed in the theoretical calculations, so that I^π_α assignments up to $E_x = 5.2$ MeV can be made on this basis.

The nucleus ^{144}*Sm.* In ^{144}Sm, feeding from negative-parity levels through the $\frac{7}{2}^-_{(1)}$, $\frac{3}{2}^-_{(1)}$, $\frac{1}{2}^-_{(1)}$ and $\frac{5}{2}^-_{(1)}$ IAR was observed recently [30]) (fig. 16). Concerning the lowest $I^\pi = 3^-$ and 4^- levels observed with a strong neutron particle-hole character, at

TABLE 7

The theoretical cross section σ_{tot} $(0^+ \to I_\alpha)$ on different IAR states to final levels I_α, compared with the experimental data for ^{144}Sm

Energy (MeV)	J^π		$\sigma_{\frac{7}{2}^-}$		$\sigma_{\frac{3}{2}^-}$		$\sigma_{\frac{1}{2}^-}$		$\sigma_{\frac{5}{2}^-}$	
	exp.	th.	exp.	th.	exp.	th.	exp.	th.	exp.	th.
3.310	$\underline{3}^-, 4^-$	4_1^-	2.84	1.14	0.32	0.01	0.28		0.42	
3.362	$\underline{3}^-, 4^-$	3_1^-	3.17	3.36	0.14	0.03	0.12		0.15	
3.393	$(\underline{3}^-, 2^-)$		0.20		0.18		0.15		0.50	
3.405	$(\underline{3}^-)$		0.34		0.25		0.23		0.28	
3.530	$(\underline{3}^-)$		0.47		0.25		0.14		0.18	
3.671	(5^-)		0.26							
3.724	$(\underline{3}^- + \underline{2}^-)$	$[3_2^-]$	0.78	[1.14]	0.44	[0.13]				
3.734	$(\underline{3}^-)$	$[3_2^-]$	0.59	[1.14]	0.22	[0.13]				
3.849	(4^-)	4_2^-	1.68	2.40						
3.869	$(4^-, \underline{5}^-)$	5_1^-	0.50	0.48						
3.890	(1^-)		0.18		0.38		0.33		0.27	
	$(3^-, 5^-)$									
3.974	$(+1^-, 2^-)$	$[2_1^-]$	0.36	[0.26]	1.04	[0.84]				
4.121	$(\underline{2}^-, 1^-)$	$[2_1^-]$	0.14	[0.15]	0.46	[0.54]	0.18		0.27	
4.245	$\underline{2}^-, 1^-$	2_2^-	0.08	0.01	1.70	0.94	0.14	0.01	0.24	0.22
4.265	$\underline{1}^-, 2^-$	1_1^-		0.01	1.58	1.46	0.22	0.14	0.31	
4.504	$(\underline{3}^-)$	3_4^-		0.05	0.18	0.11			0.31	0.12
4.607	$(1^- + 3^-)$	$\{1_3^- + 3_3^-$		0.02	0.78	0.20	0.17	0.30	0.35	0.05
				0.01		0.35				
4.716	(0^-)	0_1^-			0.10	0.05	0.28	0.10		
4.760	(2^-)	2_3^-		0.01	0.29	0.71			0.14	0.03
4.983	(3^-)	3_7^-							0.30	0.24
5.063	(2^-)	2_7^-					0.35	0.04	0.66	0.27
5.079	(3^-)	3_9^-							0.42	0.20
5.110	(1^-)	$\{1_5^-$					0.48	0.11	0.24	0.01
		1_6^-						0.13		0.04
5.156	$(\underline{0}^-, 1^-)$	0_2^-					0.54	0.25		
5.161	$(\underline{2}^-, \underline{3}^-)$	3_{12}^-							0.50	0.49
5.211	$(1^-, \underline{2}^-)$	$\{2_9^-$					0.17	0.01	0.16	0.22
		2_{10}^-								0.21

Numbers between square brackets give the probability that configuration interaction distributes the theoretical value over the indicated levels. When more than one spin is given, the underlined value is believed to be the more probable.

TABLE 8

Theoretical cross section σ_{tot} $(0^+ \rightarrow I_\alpha)$ on different IAR states to final levels I_α, compared with the experimental data for ^{142}Nd

Energy (MeV)	J^π		$\sigma_{\frac{7}{2}^-}$		$\sigma_{\frac{3}{2}^-}$		$\sigma_{\frac{1}{2}^-}$		$\sigma_{\frac{5}{2}^-}$	
	exp.	th.	exp.	th.	exp.	th.	exp.	th.	exp.	th.
3.295	$\underline{4}^-, 3^-$	4_1	3.63	2.81		0.01				
3.366	$\underline{3}^-, 4^-$	3_1^-	4.00	6.17	0.13	0.06				
3.413	(5^-)		0.44							
3.423	(1^-)		0.07		0.59	0.45	0.06			
3.574	(3^-)	$[3_2^-]$	1.50	[2.73]	0.47	[0.47]	0.10		0.55	
3.598	(5^-)		0.12							
3.705	(5^-)	5_1^-	0.83	2.09						
3.710	(3^-)	$[3_2^-]$	1.06	[2.73]	0.47	[0.47]				
3.870	(4^-)	4_2^-	3.97	5.61	0.33	0.07			0.11	
3.908	(2^-)	2_1^-	0.17	0.53	0.89	1.72		0.03	0.12	
4.117	$\underline{2}^-, 1^-$	2_2^-		0.02	2.85	1.76	0.10	0.08	0.20	
4.141	$\underline{1}^-, 2^-$	1_1^-		0.01	2.22	2.92	0.05	1.32		
4.328	$(\underline{1}^-, 2^-)$	1_2^-		0.01	0.75	0.44	0.22	0.26		
4.382	$(1^-, 2^-)$	1_3^-		0.07	0.39	0.05	0.13	1.08		
4.417	(3^-)	3_3^-		0.04	0.27	0.52		0.05	0.40	
4.495	(0^-)	0_1^-			0.10	0.15	0.28	0.49		
4.598	(2^-)	2_3^-		0.05	0.59	1.66		0.03	0.34	
4.745	$(\underline{1}^-, 2^-)$	1_4^-				0.32	0.47	1.14	0.38	
4.809	$(0^-, 1^-)$						0.53			
4.824	$(2^-, 1^-)$						0.29		0.25	
4.841	(0^-)						0.44			
4.896	(1^-)	1_5^-				0.17	0.63	0.62	0.17	

$E_x = 3.310$ MeV and 3.362 MeV, respectively, there seems to be a reversal in excitation energy as compared to the situation occurring in the lighter $N = 82$ nuclei. The qualitative agreement is again quite good, but in order to give unique assignments, comparison of experimental data with theoretical values, for partial decay widths as well as angular distributions, is necessary.

In the nucleus, on the $\frac{3}{2}^-_{(1)}$ IAR, the agreement between theory and experiment is very good (fig. 17). According to the assignment for the $I^\pi = 2^-$ (3.974 MeV and 3.724 MeV) levels, the $I^\pi_\alpha = 2^-_{(1)}$ level agrees best with the higher-lying 3.974 MeV level, which is also in agreement with the position of the corresponding $I^\pi = 2^-$ level in ^{142}Nd. The $I^\pi = 1^-, 2^-$ doublet is again reproduced, although for the $I^\pi_\alpha = 1^-_{(1)}$ level, the curving is opposite to the experimental situation. For the higher-lying $I^\pi = 3^-$ (4.504 MeV), $I^\pi = 1^- + 3^-$ (4.607 MeV), $I^\pi = 0^-$ (4.716 MeV) and $I^\pi = 2^-$ (4.760 MeV) levels, the agreement is good, which enables us to locate the different members of the $|2d^{-1}_{\frac{5}{2}} \otimes \frac{3}{2}^-_{(1)}\rangle$ and $|3s^{-1}_{\frac{1}{2}} \otimes \frac{3}{2}^-_{(1)}\rangle$ GNPH configurations in ^{144}Sm amongst the other negative-parity levels.

In the case of ^{144}Sm, even the $\frac{5}{2}^-_{(1)}$ IAR was analysed with the possibility of identifying some $I^\pi = 1^-, 2^-$ and 3^- levels in the energy region 4.5 MeV $\lessapprox E_x \lessapprox$ 5.5 MeV, with some confidence in the agreement between theory and experiment.

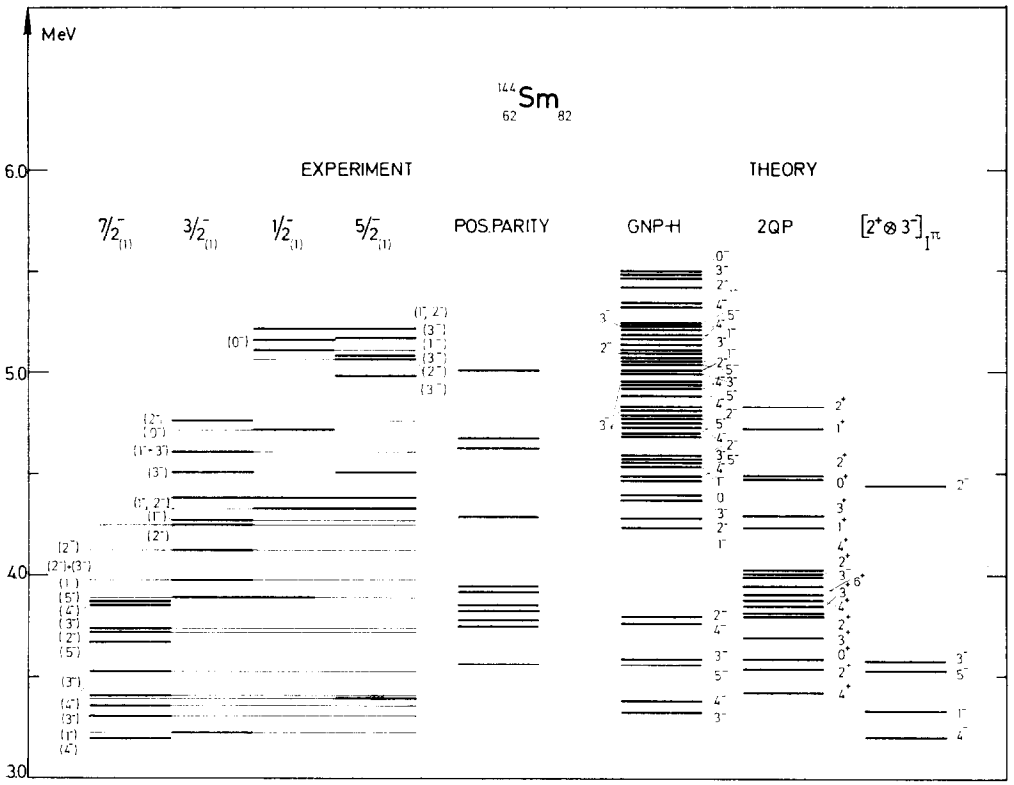

Fig. 16. See caption to fig. 6.

4.1. SYSTEMATICS OF LOW-LYING GNPH CONFIGURATIONS

By careful studying the partial decay widths and angular distributions of inelastically scattered protons through the $\frac{7}{2}^-_{(1)}$, $\frac{3}{2}^-_{(1)}$, $\frac{1}{2}^-_{(1)}$ and $\frac{5}{2}^-_{(1)}$ IAR in the doubly even $N = 82$ nuclei ^{136}Xe, ^{140}Ce, ^{142}Nd and ^{144}Sm, it became possible to locate experimentally some of the low-lying, negative-parity GNPH configuration i.e. $|2d_{\frac{3}{2}}^{-1} \otimes \frac{7}{2}^-_{(1)}\rangle$, $|3s_{\frac{1}{2}}^{-1} \otimes \frac{7}{2}^-_{(1)}\rangle$, $|2d_{\frac{3}{2}}^{-1} \otimes \frac{3}{2}^-_{(1)}\rangle$, $|3s_{\frac{1}{2}}^{-1} \otimes \frac{3}{2}^-_{(1)}\rangle$ (also $|2d_{\frac{3}{2}}^{-1} \otimes \frac{1}{2}^-_{(1)}\rangle$ in the case of ^{140}Ce, ref. [28])) (fig. 18). In the case of ^{140}Ce, the experimental assignments are unique and the agreement with corresponding, theoretical energy spacings of the GNPH multiplets is very good; although the $I^\pi = 0^-$ level is not observed experimentally. In the case of ^{142}Nd there is more fragmentation of the GNPH configurations and in some cases ($I^\pi = 3^-$) an assignment of the strongest GNPH configuration is difficult. This occurs mainly because the levels $I^\pi = 2^-$, 3^-, 4^- and 5^-, formed by coupling the collective quadrupole and octupole vibrational states to $[2^+ \otimes 3^-]I^-$, are found in the energy region of the unperturbed $|2d_{\frac{3}{2}}^{-1} \otimes \frac{7}{2}^-_{(1)}\rangle$ and $|3s_{\frac{1}{2}}^{-1} \otimes \frac{7}{2}^-_{(1)}\rangle$ GNPH multiplets [59]).

For ^{144}Sm, an analogous situation occurs with much difficulty to assign the $I^\pi = 2^-$ member, containing most of the $|2d_{\frac{3}{2}}^{-1} \otimes \frac{7}{2}^-_{(1)}; 2^-\rangle$; GNPH configuration. We assign

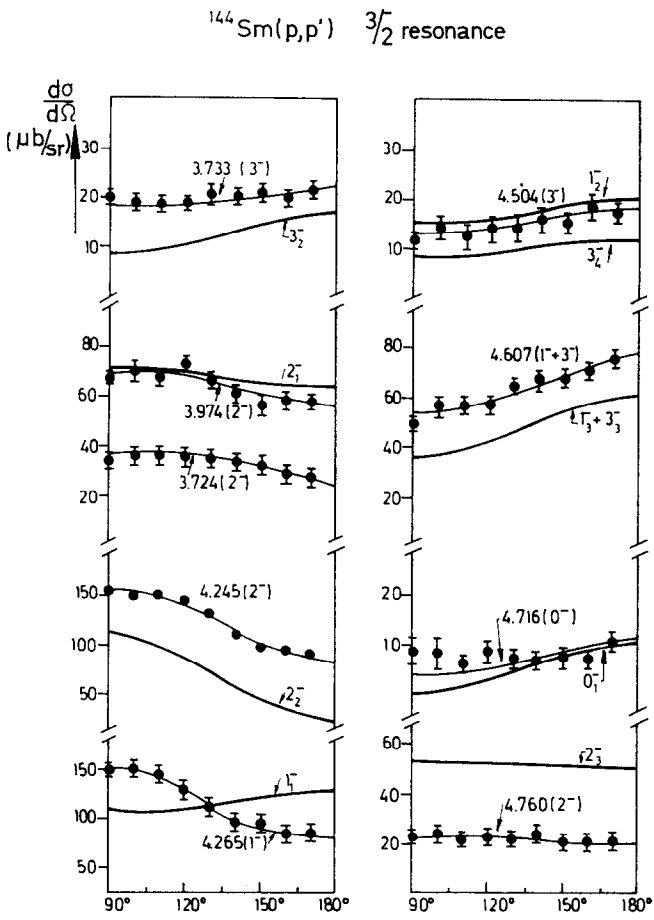

Fig. 17. Same caption as fig. 7; but for ^{144}Sm.

this to the 3.976 MeV (3^-, 5^-+1^-, 2^-) and 4.121 MeV (1^-, 2^-) levels, with also quite good agreement between theory and experiment concerning angular distributions for the $I^\pi = 2^-$ level through the $\frac{3}{2}^-_{(1)}$ IAR.

In both ^{142}Nd and ^{144}Sm the GNPH multiplets, based on the $\frac{3}{2}^-_{(1)}$ parent state of the $N = 83$ nuclei, are easily located and reproduced theoretically.

In figs. 19 and 20, the experimental and theoretical energy systematics of the lowest, negative-parity levels of definite neutron particle-hole nature are given, relative to the lowest 4^- state with strong GNPH character, for levels fed through the $\frac{7}{2}^-_{(1)}$, $\frac{3}{2}^-_{(1)}$, $\frac{1}{2}^-_{(1)}$ IAR (and also through some higher-lying IAR, if available).

The following general trends are observed:

(i) Referred to the lowest $I^\pi = 4^-$ level, a group of levels formed out of the $|2d_{\frac{3}{2}}^{-1} \otimes \frac{7}{2}^-_{(1)}\rangle$ and $|3s_{\frac{1}{2}}^{-1} \otimes \frac{7}{2}^-_{(1)}\rangle$ GNPH configuration is observed, with only very small

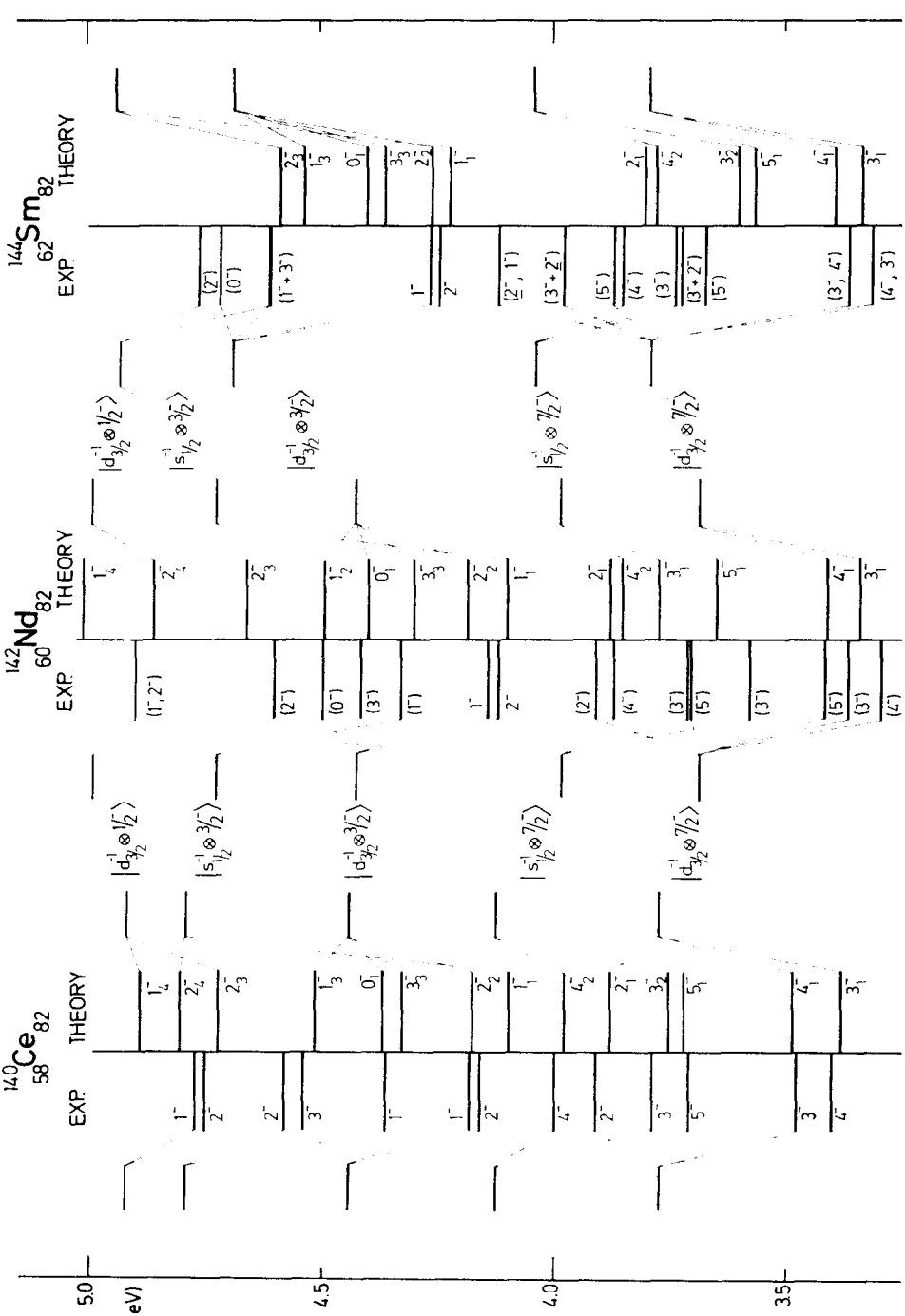

Fig. 18. Results for the GNPH multiplets based on the $\frac{7}{2}_{(1)}^-$, $\frac{3}{2}_{(1)}^-$ (and $\frac{1}{2}_{(1)}^-$ for ^{140}Ce) parent states for ^{140}Ce, ^{142}Nd and ^{144}Sm as identified among the negative-parity levels. Theoretical results are also indicated. Dashed lines are indicating the dominant GNPH configuration in a certain level $I_{(\alpha)}^{\pi}$.

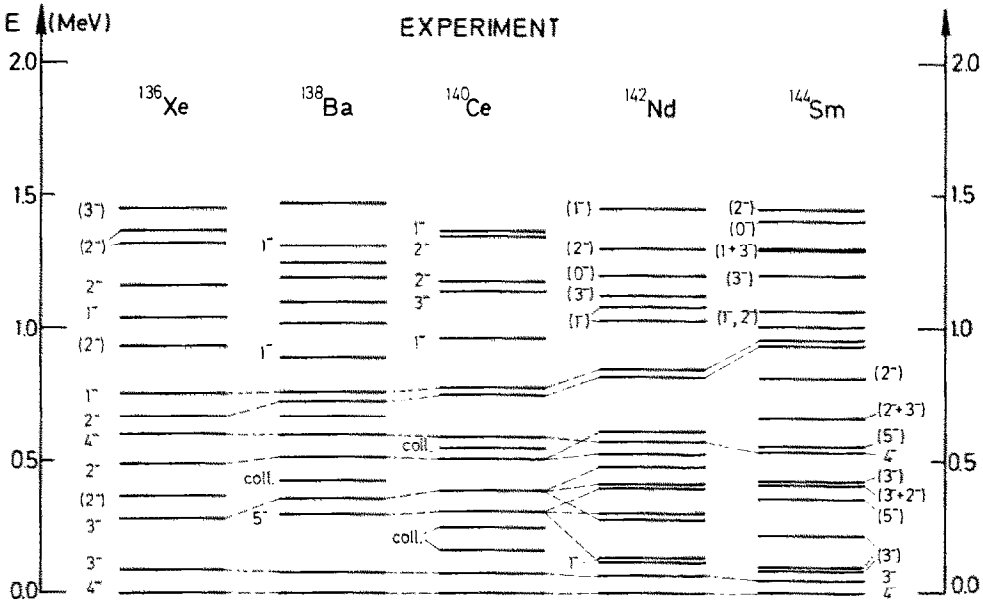

Fig. 19. Experimental energy systematics for the lower negative-parity levels in going from ^{136}Xe to ^{144}Sm, relative to the lowest $I^{\pi} = 4^{-}$ level.

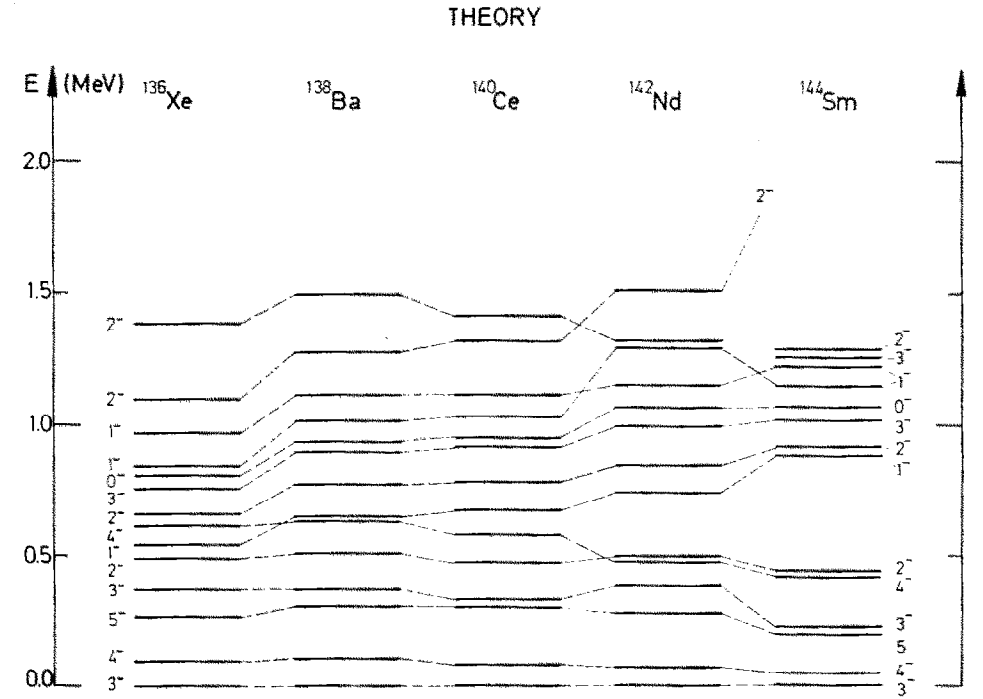

Fig. 20. Same caption as for fig. 19 but for the theoretical energy levels, and relative to the lowest $I^{\pi} = 3^{-}$ level.

changes in relative excitation energies, when considered as a function of Z. This trend is also reproduced theoretically.

The excitation energy of this $I^\pi = 4^-$ level, however, is gradually decreasing from $E_x = 3.78$ MeV in ^{136}Xe to $E_x = 3.36$ MeV in ^{144}Sm. This can be understood from the observation that the $I^\pi = 4^-$ level is mainly a $|2d_{\frac{3}{2}}^{-1} \otimes 2^-_{(1)}\rangle$ GNPH configuration. The $J^\pi = \frac{7}{2}^-$ ground state of each $N = 83$, Z nucleus mainly consists of the $2f_{\frac{7}{2}}$ neutron single-particle orbit [13-17]). The separation energy of the neutron particle in the $2f_{\frac{7}{2}}$ orbit increases faster with filling of the proton orbits than the separation energy of the neutron hole in the $2d_{\frac{3}{2}}$ orbit in the $N = 81$, Z nuclei does [33]).

(ii) A second, systematic effect is the gradual increase in excitation energy of a group of levels, in the theoretical calculation ($I^\pi_\alpha = 0^-_{(1)}$, $1^-_{(1)}$, $1^-_{(2)}$, $1^-_{(3)}$, $2^-_{(2)}$, $2^-_{(3)}$, $3^-_{(3)}$). In the experimental systematics, this Z-dependence is observed, at least for the $I^\pi_\alpha = 1^-_{(1)}, 2^-_{(2)}$ doublet. The origin of this effect can be understood, as these levels are constructed out of the $|2d_{\frac{3}{2}}^{-1} \otimes 2^-_{(1)}\rangle$ and $|3s_{\frac{1}{2}}^{-1} \otimes 2^-_{(1)}\rangle$ GNPH configurations. The first excited $J^\pi_\beta = 2^-_{(1)}$ state, as observed in the $N = 83$, Z nuclei, is mainly constructed from the collective quadrupole vibrational state $|2f_{\frac{7}{2}}, 12; \frac{3}{2}^-\rangle$, for which the excitation energy $E_x(2^+_{(1)})$ in the doubly even $N = 82$, Z nuclei, is increasing gradually with Z in going from ^{136}Xe to ^{144}Sm. This argument can serve at last for the $I^\pi_\alpha = 1^-_{(1)}, 2^-_{(2)}$ doublet as an explanation for the systematic increase in excitation energy with Z.

(iii) From the mixing between GNPH configurations, one observes the lowest $I^\pi = 4^-$ and 5^- levels to be nearly pure $|2d_{\frac{3}{2}}^{-1} \otimes 2^-_{(1)}\rangle$ configurations. The $I^\pi_\alpha = 3^-_{(1)}$ and $3^-_{(2)}$ states however, are strong mixtures of the $|2d_{\frac{3}{2}}^{-1} \otimes 2^-_{(1)}\rangle$ and $|3s_{\frac{1}{2}}^{-1} \otimes 2^-_{(1)}\rangle$ configurations, whereas the $I^\pi_\alpha = 3^-_{(3)}$ is nearly pure $|2d_{\frac{3}{2}}^{-1} \otimes 2^-_{(1)}\rangle$. The $I^\pi_\alpha = 4^-_{(2)}$ is nearly pure $|3s_{\frac{1}{2}}^{-1} \otimes 2^-_{(1)}\rangle$ and the $I^\pi_\alpha = 0^-_{(1)}$ mainly $|2d_{\frac{3}{2}}^{-1} \otimes 2^-_{(1)}\rangle$.

5. Conclusion

Inelastic proton scattering through IAR substantially extends the information on nuclear structure to higher-lying negative-parity levels in the energy region 3.0 MeV $\lessapprox E_x \lessapprox$ 6.0 MeV. These reactions have the advantage that

(i) Spectroscopic factors between excited states in both the target nucleus ($N = 82$, Z) and the parent nucleus ($N = 83$, Z) can be obtained.

(ii) Through angular distribution and partial decay-width measurements, the amplitudes and even signs for the important GNPH configurations can be determined.

In describing high-lying, negative-parity levels in the doubly even $N = 82$ isotones ^{136}Xe, ^{138}Ba, ^{140}Ce, ^{142}Nd and ^{144}Sm, and extended unified-model treatment was considered where neutron-hole states are coupled to the low-lying levels ($E_x \lessapprox 2$ MeV) of the odd-neutron $N = 83$ nuclei. Wave functions, expanded in the GNPH basis, served to calculate partial decay widths and angular distributions for inelastically scattered protons through the lowest $\frac{7}{2}^-$, $\frac{3}{2}^-$, $\frac{1}{2}^-$ and $\frac{5}{2}^-$ IAR states.

Good agreement is obtained in all cases, especially in studying the systematic behaviour of decay properties through the $\frac{7}{2}^-_{(1)}$ and $\frac{3}{2}^-_{(1)}$ resonances.

In the case of ^{142}Nd, a careful study made it possible to remove apparent discrepancies between earlier (p, p') work, performed by the Heidelberg group and more recent, high resolution work from the Montreal group.

Finally, in ^{140}Ce, ^{142}Nd and ^{144}Sm, it was possible to locate, with much confidence in the experimental level schemes, the GNPH multiplets based on the $\frac{7}{2}^-_{(1)}$, $\frac{3}{2}^-_{(1)}$ (and $\frac{1}{2}^-_{(1)}$ for ^{140}Ce) low-lying $N = 83$ levels.

The very simple picture of weak-coupling neutron hole states to the low-lying levels in the odd-neutron $N = 83$ parent nuclei is exhibited in the doubly even $N = 82$ isotones.

For the heavier isotones: ^{142}Nd and ^{144}Sm, through rapid lowering of the octupole vibrational state; the $[2^+ \otimes 3^-]_{I^-}$ levels are obtained in the energy region of the unperturbed $|2d_{\frac{5}{2}}^{-1} \otimes \frac{7}{2}^-_{(1)}\rangle$ and $|3s_{\frac{1}{2}}^{-1} \otimes \frac{7}{2}^-_{(1)}\rangle$ GNPH configurations, thus causing configuration mixing to occur and also enlarging the level density of negative-parity levels, fed through the IAR states.

A more detailed treatment, in which both GNPH, collective and 2QP proton configurations are considered in a unified-model picture in order to treat mixing more carefully is in progress [59]).

One of the authors (K. H.) is gratefull for a NATO grant which made possible his stay at Utrecht, where this study was started. He also wishes to thank Dr. A Heusler and Dr. J. P. Wurm for kindly supplying the single-particle decay widths and phases, as well as Dr. L. Foster and Dr. L. Bimbot for allowing us to make use of experimental results prior to publication.

Appendix A

The reason for describing negative-parity levels in the doubly even $N = 82$, Z nuclei in a basis where a neutron hole is coupled to the low-lying $N = 83$, Z particle states, rather than in a basis where a neutron particle is coupled to the low-lying $N = 81$, Z hole states can be given as follows:

In the $N = 83$, Z nuclei, the single-particle energy separation is given approximately by $|\varepsilon_j - \varepsilon_{2f_{\frac{7}{2}}}| \approx \hbar\omega_2$, with $\hbar\omega_2$ equal to the quadrupole phonon energy (the $I^\pi = 0^+$ to 2^+ energy separation in the doubly even $N = 82$, Z nuclei), for $(nlj) \in \{3p_{\frac{3}{2}}, 3p_{\frac{1}{2}}, 1h_{\frac{9}{2}}\}$, whereas in the $N = 81$, Z nuclei the condition $|\tilde{\varepsilon}_{3s_{\frac{1}{2}}} - \tilde{\varepsilon}_{2d_{\frac{3}{2}}}| \ll \hbar\omega_2$ is fulfilled.

A perturbation theory argument then gives for the wave functions of the low-lying $J^\pi = \frac{1}{2}^-, \frac{3}{2}^-, \frac{5}{2}^-, \frac{7}{2}^-$ and $\frac{9}{2}^-$ levels

$$|\psi\rangle = |\varphi_0\rangle + \sum_i \frac{\langle\varphi_i|H_{p\text{-}c}|\varphi_0\rangle}{E_i - E_0}|\varphi_i\rangle,$$

where the most important contribution derives from

$$|\varphi_i\rangle = |2f_{\frac{7}{2}}, 2^+; jm\rangle, \quad |\varphi_0\rangle = |j, 0^+; jm\rangle,$$

with $E_i - E_0 = \hbar\omega_2 + \varepsilon_{2f_{\frac{7}{2}}} - \varepsilon_j$, which is a very small energy ($\approx$ 0.1–0.2 MeV) in this particular case. This shows that for the states $J^\pi = \frac{1}{2}^-$, $\frac{3}{2}^-$, $\frac{5}{2}^-$, $\frac{7}{2}^-$ and $\frac{9}{2}^-$ the collective configuration $|2f_{\frac{7}{2}}, 2^+; jm\rangle$ is strongly admixed, a fact which is also observed in the experimental data: the reactions [14–18] ${}^{A}_{Z}X_{82}$(d, p) and [38, 39] ${}^{A}_{Z}X_{82}$ (p, p′)${}^{A}_{Z}X_{82}(2^+_{(1)})$.

For the $N = 81$ nuclei, however, a nearly pure single-hole state $J^\pi = \frac{1}{2}^+$ is observed as first excited state in all $N = 81$, Z nuclei [33]. Negative-parity levels in the doubly even $N = 82$ isotones, mainly constructed out of the $|(nlj)^{-1} \otimes 7^-_{2(1)}\rangle$GNPH configuration with $(nlj)^{-1} \in \{2d_{\frac{3}{2}}^{-1}, 3s_{\frac{1}{2}}^{-1}\}$ can also conveniently be described as the $|2f_{\frac{7}{2}} \otimes J^+_{(1)}\rangle$ GNHP configuration $(J^+_{(1)} \in \{1^+_{2(1)}, 3^+_{2(1)}\})$ with $J^+_{(1)}$ describing positive-parity states in the $N = 81$, Z nuclei, because the $2f_{\frac{7}{2}}$ neutron single-particle configuration is strongly present in the $7^-_{2(1)}$ $N = 83$, Z ground state. This is the case for the $I^\pi_\alpha = 5^-_{(1)}$, $4^-_{(1)}$, $4^-_{(2)}$, $3^-_{(1)}$, $3^-_{(2)}$ and $2^-_{(1)}$ states.

All low-lying levels in the $N = 83$ nuclei, except the $7^-_{2(1)}$ ground state, contain strong admixtures of the collective quadrupole vibrational state. Such states require, in the GNHP description, many configurations. Both descriptions are related by

$$|j_h^{-1} \otimes J_\beta; IM\rangle = \sum_{j_p, J', \gamma} \{\sum_{N, R} c_\beta(j_p, NR; J) k_\gamma(j_h, NR; J') \times \{(2J+1)(2J'+1)\}^{\frac{1}{2}} W(j_h J' J j_p; RI)\} |j_p \otimes J'_\gamma; IM\rangle,$$

where c_β and k_γ are the expansion amplitudes for the J^-_β and J'^+_γ low-lying levels in the $N = 83$, Z and $N = 81$, Z nuclei, respectively.

As an example, the $I^\pi_\alpha = 2^-_{(2)}$ level in ^{140}Ce, described as $-0.21|3s_{\frac{1}{2}}^{-1} \otimes 3^-_{2(1)}; 2^-\rangle$ $-0.94|2d_{\frac{3}{2}}^{-1} \otimes 3^-_{2(1)}; 2^-\rangle$ $+0.17|2d_{\frac{3}{2}}^{-1} \otimes 1^-_{2(1)}; 2^-\rangle$, decomposes in the GNHP basis into many components $0.66|3p_{\frac{3}{2}} \otimes 3^+_{2(1)}\rangle$ $-0.34|2f_{\frac{7}{2}} \otimes 7^+_{2(1)}\rangle$ $-0.28|2f_{\frac{7}{2}} \otimes 5^+_{2(1)}\rangle$ -0.25 $|2f_{\frac{7}{2}} \otimes 5^+_{2(2)}\rangle$ $-0.22|2f_{\frac{7}{2}} \otimes 3^+_{2(2)}\rangle$ $-0.13|2f_{\frac{7}{2}} \otimes 7^+_{2(2)}\rangle$. Also the $I^\pi_\alpha = 1^-_{(1)}$ level, which in the GNPH basis is nearly a pure $|3s_{\frac{1}{2}}^{-1} \otimes 3^-_{2(1)}\rangle$ level, fragmentates in the GNHP basis as $0.66|3p_{\frac{3}{2}} \otimes 1^+_{2(1)}\rangle$ $+0.40|2f_{\frac{7}{2}} \otimes 5^+_{2(3)}\rangle$ $+0.31|2f_{\frac{7}{2}} \otimes 5^+_{2(2)}\rangle$ $-0.24|2f_{\frac{7}{2}} \otimes 5^+_{2(1)}\rangle$ $+0.24$ $|3p_{\frac{3}{2}} \otimes 1^+_{2(2)}\rangle$. The lowest $I^\pi_\alpha = 0^-_{(1)}$ level, described as $0.43|3s_{\frac{1}{2}}^{-1} \otimes 1^-_{2(1)}\rangle$ -0.89 $|2d_{\frac{3}{2}}^{-1} \otimes 3^-_{2(1)}\rangle$, becomes $-0.58|3p_{\frac{3}{2}} \otimes 3^+_{2(1)}\rangle$ $-0.47|2f_{\frac{7}{2}} \otimes 7^+_{2(1)}\rangle$ $+0.32|3p_{\frac{1}{2}} \otimes 1^+_{2(1)}\rangle$ $+0.28$ $|2p_{\frac{3}{2}} \otimes 3^+_{2(2)}\rangle$.

These examples clearly show the ability to describe the negative-parity levels as simply as possible, in a scheme where neutron-hole states in the $N = 82$ core are coupled to the low-lying $N = 83$, Z nuclear levels.

Appendix B

In the case of ^{142}Nd there seems to be some disagreement between spin assignments made by the Montreal group and by the Heidelberg group, hereafter referred

to as (M) and (H), respectively. A level at 3.558 MeV, assigned as 5^-+ collective by the latter, is given as a doublet of 3.574 MeV (3^-), 3.598 MeV (5^-) by the former. Also, the 3^- assignment at 3.68 MeV (H) seems to correspond to a 3.705 MeV (5^-), 3.710 MeV (3^-) doublet. Furthermore, in the work of the Montreal group; the $I^\pi = 2^-$ level with largest $|2d_{\frac{3}{2}}^{-1} \otimes \frac{7}{2}^-_{(1)}\rangle$ GNPH configuration is found at 3.908 MeV, whereas (H) gives an $I^\pi = 2^-$ assignment to a level at 3.77 MeV and a collective assignment to a level at 3.88 MeV.

These three discrepancies, however, are due to the bad resolving power of the Heidelberg experiments and can be understood as follows;

(i) By adding the angular distributions, as observed on the $\frac{7}{2}^-_{(1)}$ IAR, to the final levels $I^\pi = 5^-$ (3.598 MeV) and $I^\pi = 3^-$ (3.574 MeV) (M) the result compares with the angular distribution corresponding to the $I^\pi = 5^-$ assignment as made by (H), (see fig. 21). A further confirmation of this statement follows because via the $\frac{3}{2}^-_{(1)}$ IAR, at $E_x = 3.558$ MeV (H), an angular distribution is obtained which agrees very well with the $I^\pi = 3^-$ (3.574 MeV) angular distribution (M), as shown in fig. 22.

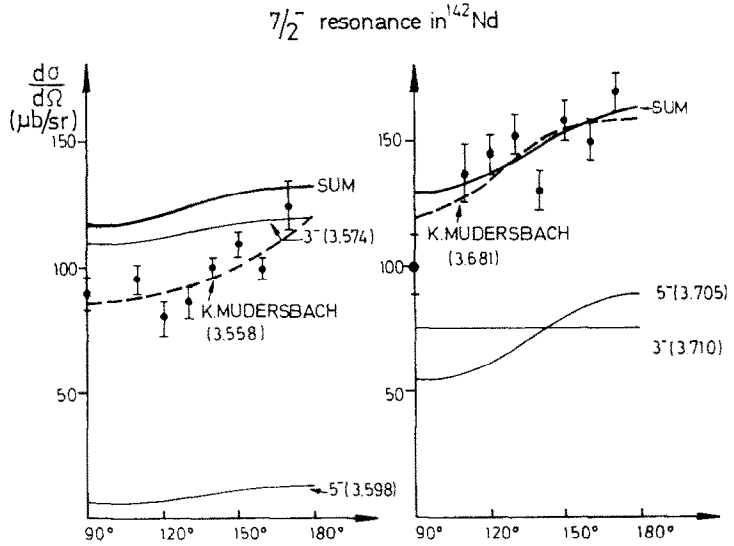

Fig. 21. Discrepancies on the $\frac{7}{2}^-_{(1)}$ IAR in ^{142}Nd. The thick full line is the sum of the separate Montreal data, whereas full lines indicate results from the Montreal group. The experimental data points and experimental fit (dashed line) originate from the Heidelberg group.

(ii) By adding the $I^\pi = 5^-$ (3.705 MeV) and $I^\pi = 3^-$ (3.710 MeV) angular distributions through the $\frac{7}{2}^-_{(1)}$ IAR, the angular distribution as measured by (H) at 3.68 MeV with an $I^\pi = 3^-$ assignment is nicely reproduced. (fig. 21).

On the $\frac{3}{2}^-_{(1)}$ IAR, only the $I^\pi = 3^-$ level is observed, with a good agreement between the Montreal data and the Heidelberg data (see fig. 22).

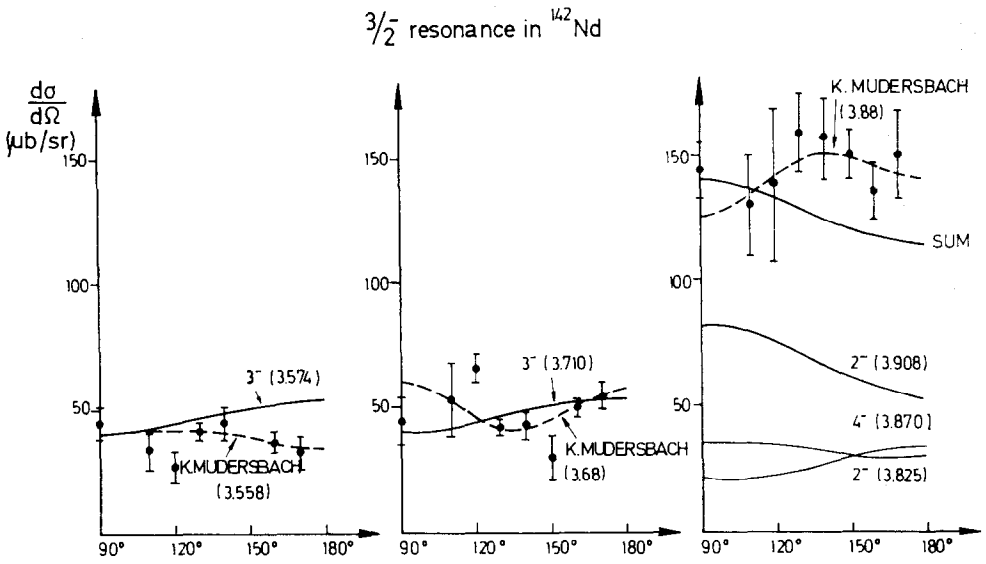

Fig. 22. Same caption as for fig. 21, but on the $\frac{3}{2}^-_{(1)}$ IAR in ^{142}Nd.

(iii) Concerning the $I^\pi = 2^-$ assignment, one can observe a very good agreement between the angular distribution through the $\frac{3}{2}^-_{(1)}$ IAR, to the 3.88 MeV level, assigned as collective (H), and the summed distribution of the 2^-(3.825 MeV), 4^- (3.870 MeV) and 2^- (3.908 MeV) levels as obtained by (M) (fig. 22).

References

1) A. Bohr and B. Mottelson, Mat. Fys. Medd. Dan. Vid. Selsk. **27** (1953) no. 16
2) G. Vanden Berghe, K. Heyde and M. Waroquier, Nucl. Phys. **A165** (1971) 662
3) P. A. Moore, P. J. Riley, C. M. Jones, M. D. Mancusi and J. L. Foster, Jr., Phys. Rev. **180** (1969) 1213
4) N. Williams, G. C. Morrison, J. A. Nolen, Jr., Z. Vager and D. von Ehrenstein, Phys. Rev. **C2** (1970) 1539
5) N. Marquadt, P. Rauser, P. Von Brentano, J. P. Wurm and S. A. A. Zaidi, Nucl. Phys. **A177** (1971) 33
6) P. Von Brentano, N. Marquadt, J. P. Wurm and S. A. A. Zaidi, Phys. Lett. **17** (1965) 124
7) L. Veeser, J. Ellis and W. Haeberli, Phys. Rev. Lett. **18** (1967) 1063
8) E. Grosse, K. Melchior, H. Seitz, P. Von Brentano, J. P. Wurm and S. A. A. Zaidi, Nucl. Phys. **A142** (1970) 345
9) G. Clausnitzer, R. Fleischmann, G. Graw, D. Proetel and J. P. Wurm, Nucl. Phys. **A106** (1968) 99
10) S. Darmodjo, R. D. Alders, D. G. Martin, P. Dyer, S. Ali and S. A. A. Zaidi, Phys. Rev. **C4** (1971) 672
11) H. L. Harney, C. A. Wiedner and J. P. Wurm, Phys. Lett. **26B** (1968) 204
12) K. Marouchian, P. Von Brentano, J. P. Wurm and S. A. A. Zaidi, Z. Naturf. **21a** (1966) 929
13) S. Fiarman, E. J. Ludwig, L. S. Michelman and A. B. Robbins, Nucl. Phys. **A131** (1969) 267
14) P. A. Moore, P. J. Riley, C. M. Jones, M. D. Mancusi and J. L. Foster, Jr., Phys. Rev. **175** (1968) 1516
15) D. Von Ehrenstein, G. C. Morrison, J. A. Nolen Jr., and N. Williams, Phys. Rev. **C1** (1970) 2066

16) C. A. Wiedner, A. Heusler, J. Solf and J. P. Wurm, Nucl. Phys. **A103** (1967) 433
17) P. R. Christensen, B. Herskind, R. R. Borchers and L. Westgaard, Nucl. Phys. **A102** (1967) 481
18) R. K. Jolly and C. F. Moore, Phys. Rev. **145** (1966) 918
19) P. A. Moore, P. J. Riley, C. M. Jones, M. D. Mancusi and J. L. Foster, Jr., Phys. Rev. Lett. **22** (1969) 356
20) P. A. Moore, P. J. Riley, C. M. Jones, M. D. Mancusi and J. L. Foster, Jr., Phys. Rev. **C1** (1970) 1100
21) G. C. Morrison, N. Williams, J. A. Nolen, Jr., and D. Von Ehrenstein, Phys. Rev. Lett. **19** (1967) 592
22) J. P. Wurm, A. Heusler and P. Von Brentano, Nucl. Phys. **A128** (1969) 433
23) K. Mudersbach, A. Heusler and J. P. Wurm, Nucl. Phys. **A146** (1970) 477
24) A. Heusler, H. L. Harney and J. P. Wurm, Nucl. Phys. **A135** (1969) 591
25) S. A. A. Zaidi, P. Von Brentano, L. D. Rieck and J. P. Wurm, Phys. Lett. **19** (1965) 45
26) P. Von Brentano, W. J. Braithwaite, J. G. Cramer, W. W. Eidson and G. W. Philips, Phys. Lett. **26B** (1968) 448
27) J. P. Wurm, P. Von Brentano and K. Mudersbach, Proc. Int. Conf. on nuclear physics, Gatlinburg, 1966, ed. R. L. Becker, C. D. Goodman, P. H. Stelson and A. Zucker (Academic Press, New York, 1967) p. 252
28) A. Heusler, Nucl. Phys. **A141** (1970) 667
29) S. Raman, J. L. Foster, Jr., O. Dietzsch, D. Spalding, L. Bimbot and B. H. Wildenthal, Nucl. Phys. **A201** (1973) 21
30) R. Martin, L. Bimbot, S. Gales, L. Lessard, D. Spalding, W. G. Weitkamp, O. Dietzsch and J. L. Foster, Jr., Nucl. Phys. **A210** (1973) 221
31) J. L. Foster, Jr., O. Dietzsch and L. Bimbot, Phys. Rev. Lett. **31** (1973) 731
32) L. Bimbot *et al.*, to be published
33) K. Heyde and P. J. Brussaard, Z. Phys. **259** (1973) 15
34) N. Auerbach, J. Hüfner, A. K. Kerman and C. M. Shakin, Rev. Mod. Phys. **44** (1972) 48
35) D. Clement, thesis, University of Erlangen, Nuremberg (unpublished)
36) H. L. Harney, Nucl. Phys. **A119** (1968) 591
37) M. Waroquier and K. Heyde, Nucl. Phys. **A164** (1971) 113
38) H. Clement, G. Graw, W. Kretschmer and P. Schulze-Döbold, Phys. Rev. Lett. **27** (1971) 526
39) H. Clement, private communication
40) J. M. Blatt, L. C. Biedenharn and M. E. Rose, Rev. Mod. Phys. **24** (1952) 24
41) A. Heusler, private communication
42) J. P. Elliott, A. D. Jackson, H. A. Mavromatis, E. A. Sanderson and B. Singh, Nucl. Phys. **A121** (1968) 241
43) D. C. Choudhury, Mat. Fys. Medd. Dan. Vid. Selsk. **28** (1954) no. 4
44) A. H. Wapstra and N. B. Gove, Nucl. Data Tables **9** (1971) 30
45) B. R. Mottelson, Proc. Int. Conf. on nuclear structure, Tokyo 1967, p. 86
46) V. Paar, DUBNA preprint E4-7454 (1973)
47) G. Alaga, in Cargèse lectures in theoretical physics, ed. M. Jean, (Gordon and Breach, New York, 1969) p. 579
48) G. Vanden Berghe and K. Heyde, Nucl. Phys **A163** (1971) 478
49) R. A. Broglia, V. Paar and D. R. Bes, Phys. Lett. **37B** (1971) 159, 257;
R. A. Broglia, R. Liotta and V. Paar, Phys. Lett. **38B** (1972) 480, and references therein
50) S. Sen, P. J. Riley and T. Udagawa, Phys. Rev. **C6** (1972) 2201
51) P. H. Stelson, Nucl. Data Tables **A1** (1965) no. 1
52) J. H. Barker and J. C. Hiebert, ORO-3398-46
53) J. T. Baker and R. Tickle, Phys. Rev. **C5** (1972) 182
54) J. van der Baarn, private communication
55) D. Eccleshall, M. J. L. Yates and J. J. Simpson, Nucl. Phys. **78** (1966) 481
56) J. H. Parker and J. C. Hiebert, Phys. Rev. **C4** (1972) 2256
57) R. K. Jolly and E. Kashy, Phys. Rev. **C4** (1971) 887, 1398
58) P. Vogel and L. Kocbach, Nucl. Phys. **A176** (1971) 33
59) K. Heyde, M. Waroquier and H. Vincx, to be published